Université de Neuchâtel
Institut de Microtechnique

Fluorescence Based Integrated Optical Biosensors

Thèse

Présentée à la Faculté des sciences
Pour obtenir le grade docteur ès sciences

par

Philipp Nicolas Zeller

Neuchâtel, octobre 2001

UFO Dissertation Band 410

Die Deutsche Bibliothek – CIP-Einheitsaufnahme
Ein Titeldatensatz für diese Publikation ist bei
Der Deutschen Bibliothek erhältlich.

Dissertation der Universität Neuchâtel
Datum der mündlichen Prüfung: 22.06.2001
Referenten: Prof. Dr. M. Koudelka-Hep
Prof. Dr. U. Spichiger
Prof. Dr. P. Seitz
Dr. R. E. Kunz

UFO Atelier für Gestaltung & Verlag GbR · D-78476 Allensbach
Internet: www.ufo-verlag.de
Erste Auflage 2002 · Alle Rechte beim Autor
ISBN 3-935511-11-6

IMPRIMATUR POUR LA THESE

Fluorescence based integrated optical biosensors

de M. Philipp Nicolas Zeller

UNIVERSITÉ DE NEUCHATEL

FACULTE DES SCIENCES

La Faculté des sciences de l'Université de Neuchâtel sur le rapport des membres du jury,

Mmes M. Koudelka-Hep (directrice de thèse) et U. Spichiger (Zürich), MM. P. Seitz et R. Kunz (CSEM, Zürich)

autorise l'impression de la présente thèse.

Neuchâtel, le 8 janvier 2002

Le doyen:

F. Zwahlen

FLUORESCENCE BASED INTEGRATED OPTICAL BIOSENSORS

PREFACE

This work was carried out in order to find new biochemical sensing schemes at reduced size as well as low cost, while improving sensitivity and selectivity. Many problems in our surrounding, the food chain and the medical care ask for appropriate sensing solutions. This work also aims to get a PhD degree in physics.
The work performed asked for a wide interdisciplinary point of view and therefore offered the opportunity to have insight into a broad variety of interesting topics within the different disciplines to be dealt with.
I estimated many people's support of different sections at the Centre Suisse d'Electronique et de Microtechnique SA (CSEM), the Institut de Microtechnique, Neuchâtel (IMT) and the Swiss Federal Institute of Technology, Zürich (Eidgenössische Technische Hochschule, ETH).
I did an interesting research work in an instructive surrounding and I had the opportunity to meet many really genius people.

All in all I can look back to an interesting yet not always carefree time. I would like to dedicate this book to all the persons who supported me during that time.

Thank you

FLUORESCENCE BASED INTEGRATED OPTICAL BIDSENSORS

CONTENTS

ABSTRACT

Integrated optical sensing chips have successfully been used for the detection of different biochemical molecules. Refractometric sensing is used for the detection of large molecules as the mass that is adsorbed onto a wave guiding material is measured. Fluorescence sensors are used for visualizing distributions of labeled molecules or to measure a concentration of molecules quantitatively by measuring the intensity of the light emitted. This method is useful especially for small molecules as drugs, antibiotics, DNA probes or ions. This work deals with new chips and new sensing schemes that have been developed and tested in order to get higher density of different recognition regions as well as higher sensitivity and lower costs. First chips have been designed and fabricated mostly in-house. The sensing principle has been demonstrated by performing standard experiments on a large laboratory set-up providing all the flexibility needed to make use of different chips as well as to evaluate different sensing schemes. Further some experiments have been performed directly detecting single stranded DNA probes, and different antibiotics in competitive assays. The results show well the effectiveness of the sensing principle described in this work even providing dynamic measurements. Dynamic means to be able to measure the whole adsorption process online in a flow cell, as the excitation of the fluorescence and the readout optics takes place on the backside of the sensor chip, opposite to the biochemistry. Notwithstanding the attainable detection limits have not been reached and exact calibration for quantification of the measured substances has not been performed, the work performed shows clearly that this way of detection may lead to a new generation of high density sensing modules at low prices providing high sensitivity and high selectivity. Ongoing work now concentretes on combining different integrated optical sensing principles in order to enhance sensitivity and selectivity again.

FRENCH ABSTRACT

Les puces de détection basées sur l'optique intégrée ont été utilisées avec succès pour mesurer différentes molécules biochimiques. La méthode consistant à mesurer l'indice de réfraction a été utilisée pour détecter de grandes molécules, car la quantité edsorbée sur la surface d'un guide d'onde est facilement déduite à partir de l'indice de réfraction. Les capteurs de fluorescence sont utilisés pour voir la distribution des molécules qui sont reconnaissables avec un colorant fluorescent. Il faut mesurer l'intensité de la lumière émise pour faire des mesures de concentrations de telles molécules. Cette méthode est prédestinée aux petites molécules, par exemple les drogues, les antibiotiques, les particules d'ADN ou simplement pour des éléments purs. Les travaux décrits ici sont basés sur des nouveaux chips et des méthodes de détection récentes qui ont été développés et testés dans le but de développer des nouveaux appareils bon marché, spécifiques et très sensibles. Les premières puces ont été dessinées et fabriquées presque entièrement par CSEM Zürich. Le principe de détection a été démontré à l'exemple des expériences standards avec un grand montage au laboratoire, ce qui laisse la flexibilité d'utiliser plusieurs puces différentes pour diverses méthodes de détection. La détection de nucléotides ADN a en plus été démontrée. De même, la détection d'antibiotiques a été faite en utilisant un essai compétitif. Les résultats prouvent l'efficacité de la méthode désignée. Des mesures dynamiques peuvent aussi être effectuées. Cela veut dire que la technique utilisée permet d'observer tout le processus d'absorption des molécules lorsqu'il se passe à la surface. Cela est possible grâce au fait que tout procédé biochimique a lieu dans une cellule fluidique d'un côté de la puce pendant que l'illumination et l'optique d'observation sont effectuées de l'autre. Et, même si les limites de détection théoriques n'ont pas été atteintes et si aucune calibration nécessaire pour les résultats n'a été faite, les travaux effectués sont un signe clair que ce genre de détection peut conduire à de nouveaux capteurs à prix réduits, offrant une grande sélectivité et une haute sensibilité. D'autres chercheurs essaient maintenant de combiner différentes techniques de détection avec optique intégrée pour améliorer encore plus les détecteurs.

GERMAN ABSTRACT

Integriert optische Sensorchips sind bereits erfolgreich für die Detektion von biochemischen Substanzen unterschiedlichster Art verwendet worden. Messmethoden, welchen die Veränderung der effektiven Brechzahl eines Lichtleiters als Mass für die Massenbedeckung der Chipoberfläche zugrunde liegt sind vor allem zum Nachweis grosser Moleküle geeignet. Fluoreszenz Sensoren werden vor allem angewendet, wenn die Verteilung von Molekülen auf einer Oberfläche visualisiert werden soll. Allerdings können mit dieser Methode auch quantitative echte Konzentrationen gemessen werden, indem die Intensität der emittierten Fluoreszenz gemessen wird. Diese Methode ist besonders für kleine Moleküle wie Drogen, Antibiotika, DNA Proben oder reine Elemente geeignet. Die vorliegende Arbeit behandelt neue Chips und neue Messmethoden, die entwickelt und getestet wurden, um Messgeräte mit höherer Messkanal Dichte sowie bessere Empfindlichkeit zu niedrigeren Preisen zu ermöglichen. Erste Sensor Chips wurden fast gänzlich im Hause entworfen und hergestellt. Das Messprinzip wurde zuerst mit standard Experimenten demonstriert, die auf einem grossen Labor Aufbau mit der nötigen Flexibilität, verschiedene Chips und unterschiedliche Messmethoden zu verwenden, durchgeführt wurden. Weitergehend wurden Messreihen durchgeführt, die einzelne DNA Abschnitte nachwiesen. Zum Nachweis unterschiedlicher Antibiotika wurden konkurrierende Reaktionen ausgelöst. Die erzielten Resultate zeigen die Effektivität der Messmethode, die dieser Arbeit als Haupgrundlage dient, und die auch für dynamische Messvorgän ge geeignet ist. Mit dynamisch wird hier die Möglichkeit angesprochen, einen ganzen Adsorptionsprozess messend mitverfolgen zu können, da der Chip in einer Flusszelle montiert ist, und die Beleuchtung ebenso wie die Detektion der Fluoreszenz von der Rückseite, wo keine biochemischen Reaktionen stattfinden, bewerkstelligt wird. Auch wenn die mit dieser Methode erreichbare Detektionsuntergrenze nicht erreicht wurde und auch eine genaue Kalibration für quantitativ exakte Messungen sich als äusserst komplex erwies, konnte mit den durchgeführten Messungen dennoch gezeigt werden, dass diese Methode zu einer neuen Generation von kleinen und kostengünstigen Mehrstoff-Messgeräten mit hoher Empfindlichkeit und Selektivität führen kann. Weiterführende Arbeiten konzentrieren sich zur weiteren Effizienzsteigerung auf Sensoren, die verschiedene integriert optische Messprinzipien kombinieren.

1 Introduction

1.1. Motivation

Many problems in our environment, the wastewater treatment, the food chain and the medical care lead to a large demand in sensors.

The quality of drinking water springs is tremendously decreasing due to contamination by pesticides and wastewater. More than a 10'000 chemical and biochemical substances considered as threatening human health are known. Many more may occur in the future or are not known. Substances that are harmful to living organisms are often very low concentrated, but they still have a huge impact on processes in an organism.

A different area of interest is the tremendous information retrieved by the genomic sequencing. A significant contribution to the technological advancement was achieved by the development of the polymerase chain reaction (PCR) [1]. Detecting DNA probes [2,3] leads to a different way of understanding known and newly appearing diseases. A main goal is to apply this understanding into faster and more accurate techniques of diagnostics and treatment. Biochemical substances wearing genetic data or different important information about diseases also often appear only in low concentrations.

These facts explain the need for accurate sensing methods in food processing and drinking water control as well as in disease diagnostics and drug development. Therefore the demand for highly sensitive sensors has strongly arisen during the last few decades and it is still raising. The goal of an accurate sensor is to detect molecules very specifically at extremely low detection limits. Specifically means that the substance of interest has to be measured exactly even in the presence of many different known or also unknown molecules. An additional challenge in developing new sensors is to make them sensitive for measuring small quantities of low concentrated substances. Further, the sensors need to get results both quickly and accurately as well as they should be cheap. New sensors have to fulfill some or all of the above requirements.

1.2. Sensors in General

Many different approaches that will not be discussed in detail here exist to detect substances in fluids or gases. There are methods as a mechanical or electrostatic filtering, different types of chromatography, mass spectroscopy, optical spectroscopy, time-of-flight or viscosity measuring, electronic and electrochemical sensors [4,5] that measure the potential, resistence or current change occuring in the presence or after a specific chemical reaction of the analyte.

1.3. Optical Sensors in General

A broad variety of optical sensors exist. They range from movement sensors to highly sensitive chemical sensors [6,7,8,9]. In order to get a (bio-) chemical sensor providing high sensitivity and selectivity it is necessary to combine a highly sensitive and selective chemical recognition layer onto an optical surface [10,11,12]. The surface behavior of an optical sensor is a very important and critical topic [13,14], as it is the place of the capturing of the substance to measure. Both, selectivity end sensitivity depend strongly on that interface, and also the optical signal information needs to be transmitted along or through that surface. The properties and the behavior of the molecules of interest lead to the sensing type and the design of the whole optical sensing scheme.

1.4. Optical Fluorescence Sensors

In optical fluorescence sensors the labeled molecules are excited by illumination with light of the exciting wavelength [15,16]. The fluorescent emission by the labels is then collected optically for detection. In conventional optical fluorescence sensors the labeled analyte molecules are illuminated directly by a beam of light. The fluorescence that is diffusely radiated into any direction around the sensor needs to be collected spatially [14]. Different optical fluorescence sensors are based on measuring the lifetime of the fluorescence [17,18,19,20,21].
Many different approaches are being tested or theoretically evaluated [22,23,24].

1.5. Integrated Optics

Integrated optics (IO) means that light is guided through waveguides of more or less complicated structures. In any kind of IO sensors different advantageous properties can be teken profit of [25,26,27]. In example miniaturized interferometers can be built [28,29,30]. But also the properties of the light guiding is influenced by the surface of a waveguide in which the light is guided quite weakly. This means that the evanescent field of the guided wave propagetes on either side of the waveguide in the substrate and the cover respectively and therefore interacts with molecules that are very close to that surface (in a sub-wavelength distance) within the range of the evanescent wave. These interactions change the guiding properties (effective refractive index, N) and thus sensors can be developed that are based on integrated optics [31,32,33,34,35].

1.6. Thesis Overview

In this thesis a new sensing approach based on integrated optics for fluorescence sensing is presented. This new approach is based on a single-pad sensing scheme. Single pad means that all the functions needed for sensing are implemented on one single pad on a sensor chip. In chapter 2 the fundamentals about integrated optical sensing are described. The new single-pad sensing scheme based on cross polarization is described and general information about fluorescence, absorption and electrochemiluminescence is given. Chapter 3 describes the material used and the methods applied within the work this thesis is based on. In chapter 4 some model experiments performing immunoassays to show the feasibility of the new approach are described and discussed. Chapter 5 describes experiments for the detection of antibiotics using the presented set-up. Measurements of DNA oligonucleotides with the presented set-up are shown in chapters 6 and 7. Chapter 6 shows the detection of the oligonucleotide tailing reaction on the sensor chip surface, while the sensing of single stranded oligonucleotides and their dehybridization on the chip is described in chapter 7. Chapter 8 presents some first experiments that have been performed combining integrated optics with electrochemiluminescence. The preliminary deposition of electrodes on a chip and their design are also explained in chapter 8. In the conclusions of this work a comparison of the presented new approach with different state of the art sensor types is made, and the present work is positioned within the field of comparable sensors research.

2 Fundamentals of Integrated Optical Sensing

2.1 Integrated Optical Sensors

Integrated optical sensors exploit the behavior of light to couple efficiently into a material of higher refractive index if the emission is very close (≤wavelength) to the surface [36,37]. Also the fact that molecules adsorbed within this range influence the evanescent field of a guided wave is used for sensors [25]. In refractometry this last fact is used as any mass adsorbed to the surface of a waveguide changes the effective refractive index and thus the coupling angle of the propagated light via a specific grating coupler on the waveguide. This sensing method is very suitable for the detection of large molecules, as it is a measure of the surface mass density. Each molecule bound to the recognition layer on the sensor chip clearly contributes to the total mass adsorbed to the waveguide surface. Even very small changes of the effective refractive index (N) result in a different k-vector of the guided mode and thus in a different coupling angle at a grating coupler of a specific grating constant. Even more accurate measurements can be performed eliminating the need of scanning angles if slightly chirped gratings are used. Observing at a constant angle leads to a shift of the coupled signal (Integrated optical light pointer, IOLP, [38]) in the y-axis where it is coupled through the appropriate grating constant. So the total amount of adsorbed molecules can directly be measured by the use of a converting look-up table. There is no need to label them with fluorescent dyes or different recognition markers when measuring using the method of refractometry. Replicated integrated optical (IO) sensors based on planar waveguides have successfully been used for refractometric immunoassay measurements [39 - 46].

2.2 Fluorescence

Other methods are necessary however for the detection of processes leading only to small changes in the surface mass density. For example if low concentrations of small molecules like drugs have to be measured. In this case, assays making use of molecules that are labeled with a fluorescent dye are well adapted [14,47]. Various types of integrated optical sensor schemes based on fluorescence, fiber optical [22,48] as well as planar optical sensor types have been presented earlier [49 - 63]. For future applications, it is important to reduce the cost of the sensor chips and of the whole system as well as to increase the density of the sensing pads on a single chip for multi-component analysis and/or for achieving an enhanced specificity or accuracy (for example for diagnostic tests).
The conventional sensing schemes of integrated optical fluorescence sensors based on planar waveguides use separate regions on the chip for light input/output and sensing.

In integrated optical fluorescence sensors the evanescent field of the illuminating light propagating in the waveguide excites the adsorbed labeled molecules. The emitted fluorescence light is then coupled efficiently into the same waveguide and coupled out via a grating pad at a

different angle than the excitation light. This method is very convenient for detecting small molecules such as drugs, heavy metals or ions. As the molecules to be detected have to be labeled with fluorescent dyes it often is necessary to perform competitive assays. That means that the quantity of analyte molecules is measured indirectly. Fluorescence can be used to visualize distributions of molecules or to simply show their presence. Quantitative detection by fluorescence light intensity measurements asks for extremely accurate calibrations.

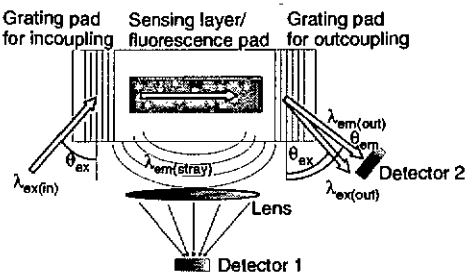

Figure 2.1: Conventional fluorescence sensing schemes based on two or three separate pads depending on the scheme of light collection.

The conventional schemes that are commonly used for fluorescence sensors consist of at least two different pads. Figure 2.1 shows how the excitation light is coupled into the waveguide by a grating pad. Then, the light is propagated in the planar waveguide for illuminating the molecules bound to the sensing layer on the chip surface by its evanescent wave. The emitted fluorescence light is then either directed to detector 1 by a lens or collected by the waveguide and coupled out to detector 2 by a second grating. As the wavelengths of excitation λ_{ex} and emission λ_{em} differ, the corresponding outcoupling angles are different. The difference of the two outcoupling angles however is small and makes it in this conventional arrangement very difficult to separate the signal from the excitation light geometrically. This means that the exciting light has to be weak enough in order to fade by exciting the fluorescent dyes, or an optical bandpass filter has to be used for reading out the fluorescence light coupled out via the second grating. If multiple sensing areas are used in a series also losses of excitation light by propagation as well as from having excited fluorescence may occur. Therefore, one big advantage of the scheme presented here is that each detection point is practically independent from the others, which is not the case in other approeches [64].

2.3 Cross Polarization

In this work, a new approach is demonstrated. The emphasis is on two aspects, namely (1) to lower the chip costs by making use of replication techniques, and (2) to reduce the real estete needed on the chip surface by introducing a single-pad sensing scheme [65]. This means that a single-pad grating coupler provides the whole functionality of a sensing unit. The new compact single pad integrated optical fluorescence sensing method is dedicated for quantitative detection if all the used parts are

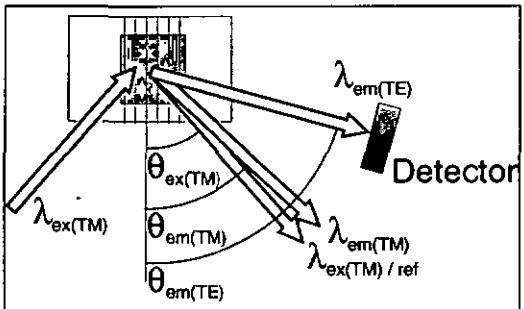

Figure 2.2: Single ped fluorescence sensing scheme including illumination, excitation end readout.

identically produced and set up. The principle is based on a planar dielectric waveguide containing multiple - sensing units, each consisting of a single-pad grating coupler structure as shown in figure 2.2.
In this single-pad scheme all the following functions are incorporated in one single pad: input of the laser light, excitation of the labeled analyte molecules, efficient collection of the emitted fluorescent light in the wave-guide, background suppression, and coupling of the guided wave out to the detector. The advantage is to save space within the sensing set up and to prevent the fluorescence from propagating through the waveguide thus losing intensity. The results demonstrate a high efficiency of the fluorescence light excitation and collection as well as a good suppression of the volume background. Figure 2.3 shows a schematic representation of the measuring principle whereas figure 2.4 schematically shows the meesuring set-up. The sensor chip forms the transparent window of a fluidic cell. In the center, a grating coupler strip is located and multipe spots for multiple measurements on this strip ere illuminated by means of a laser diode using time-multiplexing. Two single-pad channels are explicitely shown, namely a sensing (S) and a reference (R) ped. The fluorescence light emitted by labeled molecules adsorbed on the chip surface is coupled out to a single detector (photomultiplier tube) for all the spots. For a better background suppression, the fluorescence light is observed via the TE_0 waveguide mode, while the excitation is performed

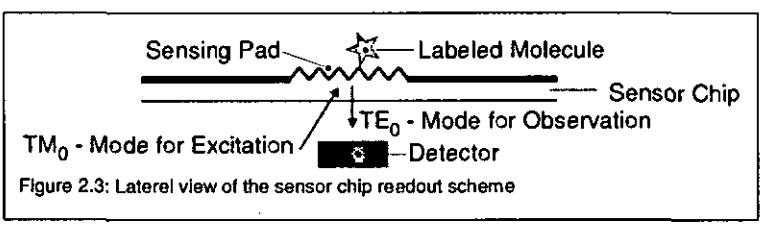

Figure 2.3: Laterel view of the sensor chip reedout scheme

via the TM_0 mode.

The molecules that have been adsorbed to the sensing layer, being a part of the same pad the grating is located at, ere therefore illuminated by the evenescent field of the planar wave as well as by the laser beam directly.

Their fluorescent light is being collected by the waveguide, exciting both a TM- and a TE-polarized mode.
These modes are immediately coupled out again by the same grating. And so is the TM-polarized mode of the exciting laser that is coupled out at the very same angle as the laser beam is reflected to. This high intensity of light together with the small difference between the outcoupling angles makes separation of exciting light and fluorescence signal at the same polarization nearly impossible.

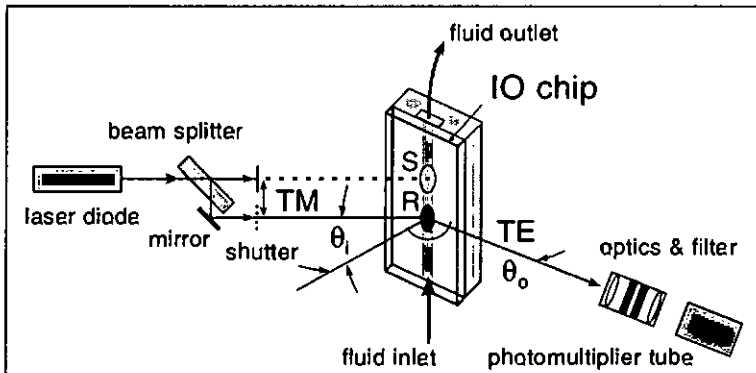

Figure 2.4: Single pad fluorescence sensing scheme including fluidics, illumination, excitation and readout.

Making use of efficient transfer of radiation directly from the near field of the dye molecules via evanescent waves to the TE_0 waveguide mode, and observing the corresponding output beam can markedly improve this situation. This approach is based on the fact that fluorescent molecules can radiate very effectively into an optically denser medium if they are located very close (<< one wavelength) to the low/high index interface [36]. In our case, we do not only make use of this enhancement for the illumination of the dye molecules (via the TM mode), but also, at the same time, for the detection of the emitted radiation (via the TE mode). Furthermore, the TE-polarized mode of the fluorescence signal is coupled out at a very different angle of $\theta_{em}(TE) = 64°$ whereas just a negligibly small part of the TM-polarized exciting light turns into a TE-polarized mode in the waveguide coupling out at $\theta_{ex}(TE) = 66°$. In addition to the better angular (and polarization) separation, a better discrimination of the radiation emitted by the molecules immediately adsorbed to the recognition layer versus the dye molecules present in the bulk medium, results from this approach.

In order to suppress the additional background originating from the plastic substrate's fluorescence and the scattered light from the replicated gratings, and therefore to further improve the signal-to-noise ratio, an additional optical band pass filter is used. This markedly reduces this

background when the coupled-out fluorescence signal is directed to the detector by imaging optics.

2.4 Absorption

Instead of exciting fluorescence the remaining intensity of the illuminating laser light can be measured if an absorbing layer is coated onto the chip [66,67,68,69]. Measurements based on this method have not been performed within this work after first tests did not show satisfying results.

2.5 Electrochemiluminescence

A modification of integrated optical sensing is measuring electrochemiluminescence via a dielectric waveguide. A current applied to microelectrodes in the fluid stimulates the accordingly labeled molecules and excites electrochemiluminescence [70,71]. If this luminescence is emitted close enough to the dielectric surface it is coupled into the waveguide and guided to the grating coupler, from where the signal can be directed to the detection module the same way as the fluorescence signal. Some tests using this scheme have been performed.

3 Materials and Methods

3.1 Chips

The sensor chips have been fabricated in the following way.

- Chip Design

First, the grating period (Λ) required providing suitable coupling angles was calculated. For the design of a chip two main parameters have to be taken into account carefully in order to get efficient sensors. These are the properties of the waveguide and the grating coupler (optical) on one hand as well as the layout of the sensing channels (geometrical) on the other.
The waveguide material and its thickness are the main parameters defining the range of the effective refractive index of the sensor. In relation to the preferably used laser wavelength the constant Λ of the grating coupler shall be chosen to lead to useful coupling angles for illumination as well as for read out.
The wave guiding film materials used given by technical processes were Titanium dioxide and Tantalum pentoxide (only glass chips).

- Grating Constant

The grating period (Λ) must be calculated to get angles for illumination and detection that are practical by means of the mechanical measuring set-up considering the wavelengths that will be used. Further a good separation between the excitation wavelength and the emitted signal is requested. The grating constant that was chosen for the standard chips was 600nm (The periodicity (Λ) of the produced chips was 595nm), as the calculated coupling angles for this grating in a TiO_2 waveguide of 160nm thickness at 658.1nm (wavelength of used laboratory set up laser diode) were calculated to be

TM +51.8°
TE +69.8°
Fluorescence (maximum at λ = 670nm, mean around 690nm):
TM +45.7°
TE +67.8°

The calculation was performed respecting the coupling condition (3.1.1): A plane wave u_l at the wavelength λ illuminates the grating at an angle of incidence θ_l measured in the ambient medium A with refractive index n_a=1 (air). If the grating coupler resonance condition is fulfilled, a guided mode u_m is excited with maximum coupling efficiency.

$$N = n_a \sin\theta_i + m_g \lambda/\Lambda \quad (3.1.1)$$

where Λ denotes the periodicity of the grating (grating constent) and m_g the grating diffraction order.
The effective refractive index N is defined by (3.1.2):

$$N = k_z / k \equiv \beta / k \quad (3.1.2)$$

where $k=2\pi/\lambda=\omega/c$. Here, c denotes the speed of light in air and ω stands for the corresponding angular frequency. The direction z is defined as the propagation direction of the mode within the waveguide. The meaning of N is very fundamental in integrated optics; it depends on the wavelength λ, the polarization of the light and on the waveguide parameters (thickness of the wave guiding film, thickness of a (biochemical) recognition layer (L) on

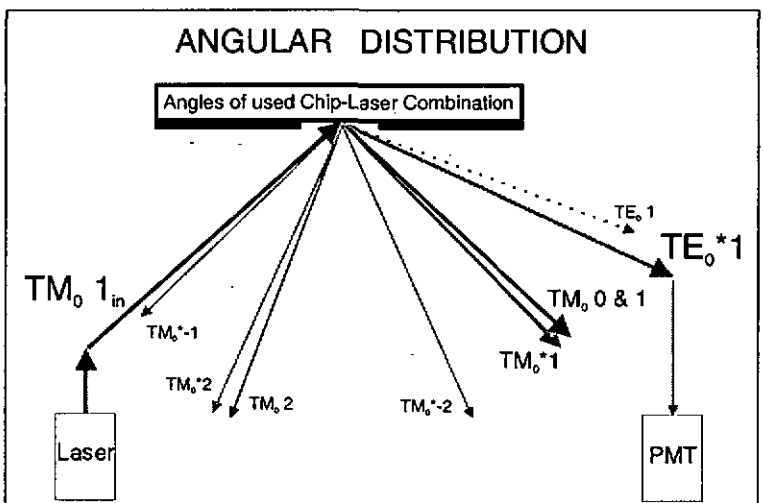

Figure 3.1: Angular distribution of the TiO_2 waveguide on a replicated chip used if illuminated at 658.1nm and emitting fluorescence at 690nm.

the waveguide surface, n_C, n_F, n_S, n_L, which themselves depend on the wavelength λ). N can not be expressed by an analytical formula. Rigorous numerical calculations of finite gratings are a very complicated and yet to be solved topic. [72]

Figure 3.1 shows the angular distribution given by the used polycarbonate chips with TiO_2 waveguide.

- Fabrication of replicated Chips

The processing of the chip production starts fabricating a silica master into which a grating pattern is transferred photolithographically. Pieces of e quartz plate (Corning) of 1mm thickness were used. After a careful

cleaning procedure the SiO_2 sample was spin coated by anti reflection coating (ARC XL-20, Brewer Science Inc.) in order to prevent internal reflections of the holographic signal to be applied later. The spin coating of ARC was done two times for each sample for getting a good non-reflective surface. Spin coating of the ARC layer onto the sample was done by spinning the plate with the applied drop on top for one minute at 2000RPM and then drying the layer by heating it up to 180°C for another minute. Repeating this procedure but heating only at 160°C led to an acceptable enti reflectivity. Third layer to be applied was the photo resist (Microposit S1805). It was spin coated by accelerating at level 5 to the initial rotation speed of 500RPM for 2 seconds and then accelerating at level 3 to the final rotetion speed of 4000RPM for another 35 seconds. Drying the photo resist was reached by heating the sample to 115°C for one minute.

Then a corresponding interference-grating pattern was generated on a holographic set-up using a He-Cd-laser (Liconix, $\lambda = 441.6nm$). This laser was split up into two identical beams that interfere at a specific angle in order to generate interference lines of the width needed (minima and maxima of the period Λ. The silica master coated with photo resist is placed into this interfering plane. The quartz sample was exposed to this holographic interference grating for between 2 and 8 minutes (used standard was 350 seconds). The exposure time defines the duty cycle of the grating lines in the photo resist and therefore later in the chip material. The light coupling efficiency of the grating depends on the shape of the grating as well as on its duty cycle.

After exposure the photo resist had to be developed in a standard developer (Microposit 303, 1:10), which had to be stirred well immediately before each use. Developing was done for 20-25 seconds in order to fix the sinus like volume grating structure. After developing the sample was rinsed with de-ionized water for at least one minute.
Next processing step is vapor deposition of e 4nm thin chromium layer at an angle of 14°. This builds up a non-continuous triangular structure on top of the photo resist grating.

The grating pattern of photo resist, covered by chromium, was etched into the silica master by oxygen plasma etching. Only the chromium layer could prevent the photo resist from flattening down too quickly and so not transferring the line structures into the hard quartz underground.

The macroscopic structure of the grating pads was defined using an eluminum shadow mask. Grating stripes of 1mm width were repeatedly placed on the master to provide multiple chips from every single fabrication step (See figure 3.2).

The master was then used to fabricate a negative nickel shim by electroplating techniques. Electrodes were mounted on the gold sputtered quartz master for growing a nickel shim by electroplating. To finally produce the replicated chips, the shim was used as a negative master to replicate the grating structure into 250µm polycarbonate sheets (Röhm). The replication was done by embossing the structure of the quartz master

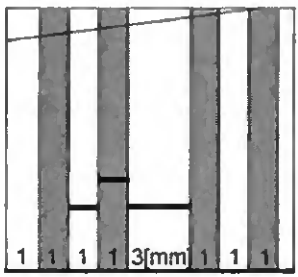

Figure 3.2: PC chip layout with pairs of 1mm wide greting stripes. (left)

Figure 3.3: photograph of a replicated IO sensor chip. (right)

from the nickel shim into a polycarbonate (PC) sheet during 4.5 minutes at a pressure of 4.5 bar and at a temperature of 240°C. After cooling the nanostructured polycarbonate chips have been sent to Unaxis Balzers AG for waveguide deposition. A TiO_2 waveguide with a thickness of 160nm and a refractive index of 2.4 was deposited onto the plastic substrates in a standardized sputtering process of Unaxis. This process begins applying a layer of about 10nm SiO_2 onto the PC substrate. After that the TiO_2 is sputtered onto the chip. Only this process leads to the needed efficiency of wave guiding. This process cannot be performed for Ta_2O_5 coatings onto PC as Ta_2O_5 requires a higher temperature. Optically TiO_2 (n=~2.4) is more interesting than Ta_2O_5 (n=~2.1) because of its higher refractive index. Biochemists however often prefer Ta_2O_5 because of its higher stability and inertness. More details on the single fabrication steps are available in Ref.[38].
Figure 3.3 shows a photograph of such a chip.

- Polycarbonate (PC) chip substrate – vs. – Glass chip substrate

Many differences between glass chips and (replicated) PC chips have been observed.
As an advantage of PC chips the costs and the possibility of cheap mass production must be mentioned first. One single nickel shim can be used for embossing thousands of (theoretically) identical low cost plastic chips.

But in the time being many disadvantages of plastic chips have arisen thus motivating to change completely to glass chips. Especially now as a process line has been set up at Unaxis Balzers AG to build glass chips with actually identical grating structures in an automatic way.

Figure 3.4 shows the angular distribution of these glass chips that were typically used towards the end of this work. Figure 3.5 is the scheme of their layout that was designed towards multi array sensors.

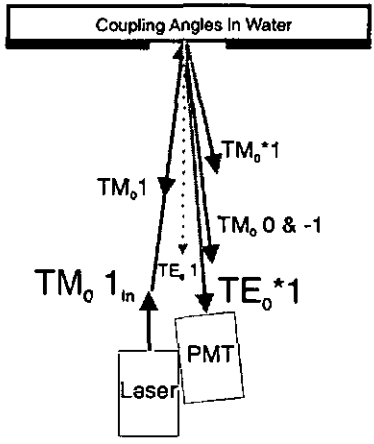

Figure 3.4: Angular distribution of the Ta_2O_5 waveguide on a glass chip used if illuminated at 658.1nm and emitting fluorescence at 690nm.

Disadvantages of plastic chips are

- Auto-fluorescence
- Non-stability of the substrate due to pinholes in the waveguide sensitivity of PC to aggressive solutions as solvents and acidic solutions.
- The wave guiding film does not adhere well.
- Possibility of applying TiO_2 waveguides only
- Non reproducibility of the gratings caused by slightly varying pressure and temperature during the embossing

The differences between the PC chips and the glass chips are obvious. The gratings of the glass chips as reproducible as also the grating depth and grating constant. This leads to more accurate coupling angles within constant conditions (wavelength, polarization, fluid) than for the PC chips, except some rare bad coating runs at Unaxis showing a slight gradient in the waveguide thickness. This little processing problem also showed up sometimes when coating PC chips and is not at all a typical problem of glass substrates. The glass is much more stable to many kinds of fluids, so the substrate is not dissolved and thus the waveguide does not dissociate. Further the glass chips are much more planar and smooth on the surface and besides that do less fluoresce themselves.

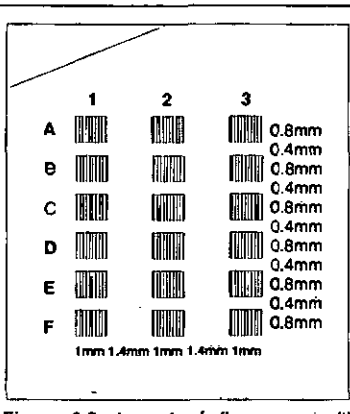

Figure 3.5: Layout of the new multi greting-pad glass chip

- Reasons for Change

The bad reproducibility of the hot embossed gratings, the sensitivity of PC to acidic solutions as well as the strong scattering of light and self fluorescence by the PC chips led to the decision to change definitely to the new glass chips.

- Characterization

To characterize the properties of the waveguide and of the grating the chips were illuminated with different lasers (He-Ne 632.8nm, He-Cd 441.6nm) and the first diffraction angles was measured in autocollimation. That means the beam of the first diffraction order rediates back to the laser source. The general diffraction equation for reflecting gratings

$$\sin \theta_{out} = - (m_g \lambda / \Lambda + \sin \theta_i) \qquad (3.1.3)$$

is then reduced by the fact that $\theta_i = \theta_{out}$ of the first diffraction order (m_g=1), and the grating constant is calculated by:

$$\Lambda = \lambda / 2\sin \theta_i \qquad (3.1.4)$$

Where Λ is the grating constant, λ is the laser wavelength, m_g is the diffraction order and θ_{out} is the angle of diffraction.
Further, the coupling angles of the gratings for the TE and the TM polarized mode have been measured in air or in water on the set up illuminating with the same laser used for experiments. Measuring the light intensity at the edges of the waveguide during an angular scan results in e typical resonance curve as shown in figure 3.6. Therefore glass fibers were connected to the edges of the waveguide. These fibers led to photodiodes to measure the brightness peaks at the coupling angles.

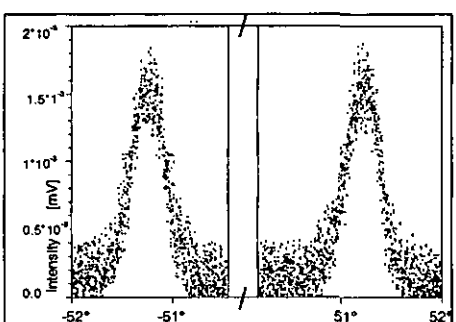

Figura 3.6: An angular scan shows the exact coupling angle of an individual PC chip and thus is used for characterization and quality control. Measured at the edges via a fiber.

The same type of angular scans were repeatedly performed at a small angular range during measurements in order to assure that the chip be illuminated at the angle of optimum coupling. This is necessary as temperature or pH changes may result in a variation of the coupling angle. Figure 3.7 shows how this was measured.

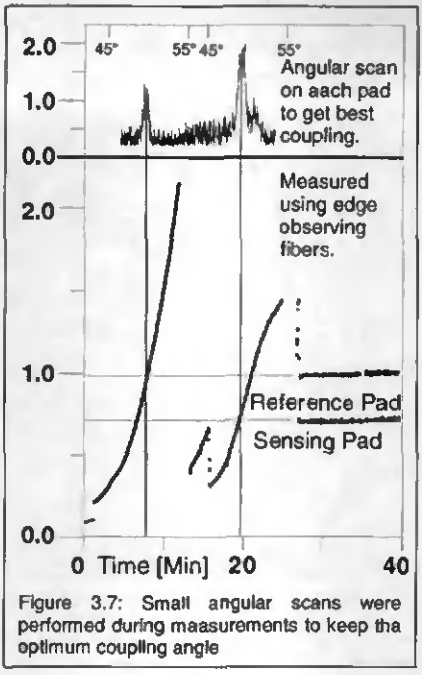

Figure 3.7: Small angular scans were performed during maasurements to keep tha optimum coupling angle

- AFM, SEM, Fluorescance-Microscopy

Some of the replicated PC chips as well as some of the quartz masters were controlled in the etomic force microscope (AFM, Figure 3.9) and, after sputtering a thin gold layer to the surface, in the scanning electron microscope (SEM) in order to characterize the submicroscopic grating structure. Herein the form of the greting could be observed. A nearly but – obviously – not perfect rectangular grating structure with rounded edges could be observed. Further the gratings depth, constant and the duty cycle could be measured. Figure 3.8 is the image of a grating structure obtained by an SEM.

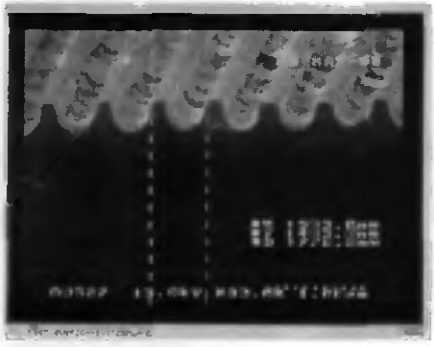

Figure 3.8: SEM imaga of embossed grating structure provides information of the grating constant, duty cycle and quality

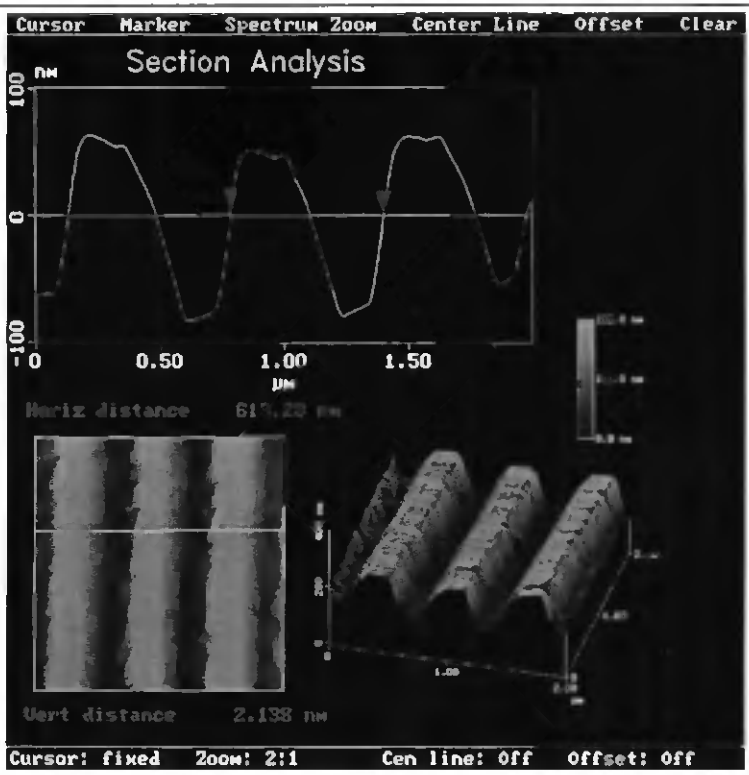

Figure 3.9: AFM image of embossed grating structure.

3.2 Sensing scheme and experimental set-up

- Single Pad

In order to reduce the peth of the guided wave as well as the whole chip size Compared to the conventional integrated optical sensing schemes described in chapter 2.2 and in respect to later multi channel sensing a new single pad sensing scheme was designed as it was described in chapter 2.3.

- Cross Polarization

Using single pad fluorescence sensor chips makes it more important to separate the illuminating light from the fluorescence signal. That is because the exciting laser light is reflected and scattered on the very same pad where the emitted fluorescence light originates. This is achieved for example by measuring only the cross-polarized portion of the fluorescence. The illuminating laser beam is linear polarized whereas the fluorescence usuelly is not polarized [*]. Therefore the emitted

fluorescence propagates in the waveguide in at least two different modes in each direction, the TE_0 as well as the TM_0 mode. Both of these guided modes are coupled out at different angles. The illuminating light exciting the fluorescent dyes was usually TM polarized. The angular difference between exciting light and emitted light caused by the slight wavelength shift was small.

In all the experiments that were performed for this work (except chapter 8, ECL) the intensity of the fluorescence excited by an illuminating laser was measured. Therefore much effort was to be done for suppressing the laser light by detecting the signal. This was done using different suppression techniques.
That is:

- Different coupling angles due to different wavelengths
- Measuring only the cross-polarized portion of the fluorescence
- Using a band pass filter

[*] It can be assumed that specific dipole molecules, if specifically bound to a surface, emit polarized light, especially if they are excited by a polarized light source. This is only the case if the binding prevents moving [73] as in crystalline structures, where the degrees of freedom are limited.

In the sensing scheme used for this work the exciting laser beam was most of the time TM-polarized. It was emitted by a 658.1nm laser diode and mechanically chopped in order to allow lock-in amplification. This light was coupled into the planar waveguide on the sensing pad grating at the angle of the first grating coupling order. Using a 160 nm TiO_2 film and a grating constant of 595nm leads to an angle $\theta_{ex}(TM) = 52°$.

- Second Order

In order to get a better separation between the exciting laser light that also is coupled into and propagated through the waveguide to be coupled out at its specific coupling angle, and the emitted fluorescence, which is coupled out at a slightly different angle due to the shift in the wavelength, measuring the intensity of the fluorescence at the angle of the second coupling order was considered. Many measurements performed did not show clear signals for a long time. This was caused by two different reasons:
First, the second order, only couples via not sine shaped gratings due to total destructive interference in sine shaped gratings. Only an asymmetric duty cycle increases the efficiency of the second order.
Second, the coupling angle of the second coupling order coincides with the second diffraction order of the grating. This can be derived using equations 3.1.1 to 3.1.3.

So the resonance peak was below the second grating diffraction order signal of the illuminating light and thus not detectable.

- Using an optical band pass filter

As the illuminating laser generates a lot of light scattering as well as different kinds of reflections, and control light's background light was present, an optical filter was used in front of the photo multiplier tube to additionally suppress as much background as possible. The filter was the emission filtering part of an exciter/emitter set by Omega Optical (XF70 690 DF40) and had a pass band region from about 670nm up to 710nm.

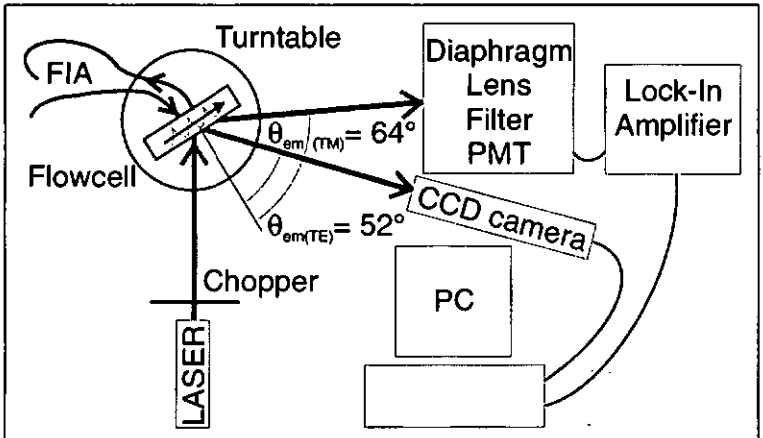

Figure 3.10: Experimental set-up for fluorescence measurements.

- Experimental Set Up

Figure 3.10 shows an overview of the set-up used for IO fluorescence measurements. It consists of the flow cell mounted on a turntable containing the IO sensor chip (see figure 3.11). The chopped illuminating laser beam can be shut in order to reduce photo bleaching of the fluorescent dyes during the adsorption phase. It can also be split into spatially different parts to provide multi analysis measurements using multiple single-pad units on one chip.
Adjustment of the chip position is done using three linearly moving tables and the turntable. Optionally the sensing chip can be monitored using a CCD camera. Turntable angle and readout optics geometry can accurately be adjusted as well in this set-up. Even online adjustments can be performed by means of an optional detector in order to readjust the optimum coupling-angle. The TE-polarized part of the emitted fluorescence light, propagating a separate TE mode in the waveguide, is coupled out of the waveguide by the grating structure. A diaphragm and a lens provide an image of the sensing pad via a band pass filter to the detector, a non-cooled photo multiplier tube. No photon counting is used. Implementing that technique would however increase the sensitivity, but

also the size and the cost of the setup. The photocurrent is changed into a voltage and lock-in amplified prior to analysis.

- Optical Table

An optical table (TMC) having a large mass that is damped with nitrogen and provided with screw holes in 5cm intervels was used as basis for the experimental set up. The setup itself provides a broad flexibility to perform different types of experiments at different angles and using different laser sources. Three lasers are implanted, one of them, a laser diode at a wavelength of 690nm, used to adjust the readout optics of the fluorescence emission as it is at the same wavelength. A turntable with different mounting arms for all kinds of optical elements is the center of the

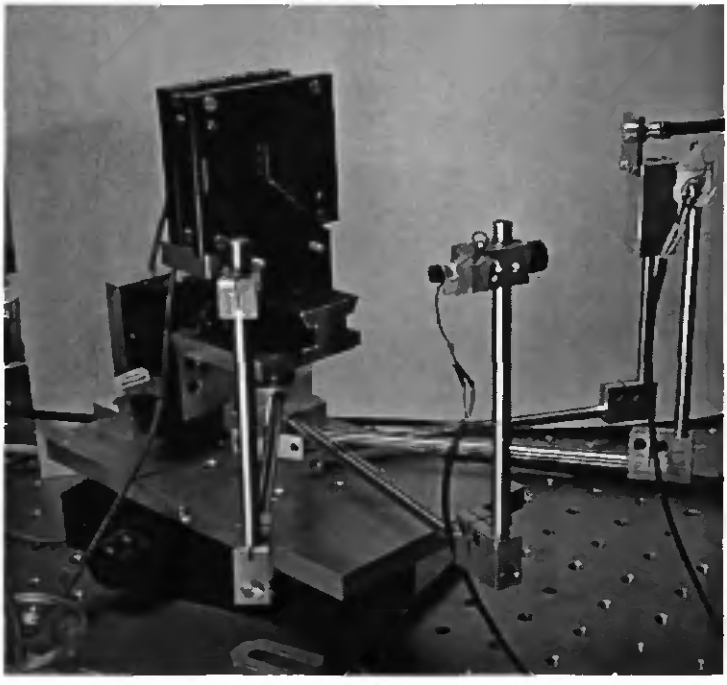

Figure 3.11:
The flow cell mounted on the turntable is the center of the measuring set-up.

set up. The chip is held on top of this turntable, mostly being mounted in a flow cell. A detailed view of the flow cell holding the IO sensor chip is shown in figure 3.12. The fluidic back plane can be connected with tubes to the flow injection analysis (FIA) system. All fluids as buffer and analyte containing sample are pumped through the connections in the back plane to the reaction volume, which is in direct contact with the bio-coated chip.

Fluidics are driven by two peristaltic pumps and two multi-way valves. The active chip area is illuminated from the opposite side passing through the chip's substrate. The laser beam therefore never needs to pass across the volume containing the analyte molecules prior to interacting with the chip. This means that the light is not undergoing unwanted changes.

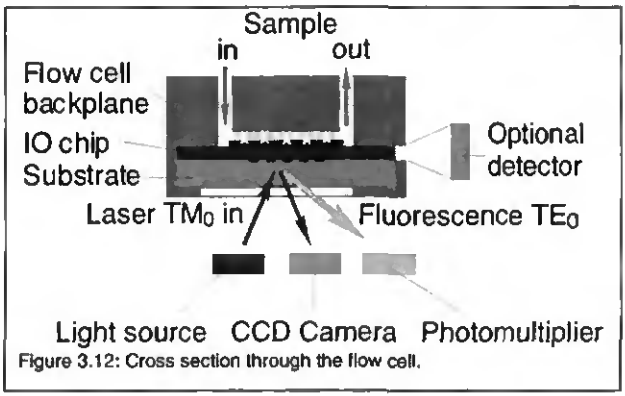

Figure 3.12: Cross section through the flow cell.

- Measurement Tools

All the measurements - except the resonance detection scans observing via the edges of the waveguide - have been performed using a photo multiplier tube (PMT, Hamamatsu H-6240-01). The PMT for signal detection was mounted on one of the turntable arms providing the possibility to be fixed on the optical table if an angular shift between the sensor chip and the readout optics was needed. The photocurrent was changed into a voltage and amplified in a lock-in amplifier (Stanford Research SRS30). Therefore the illuminating light source was chopped mechanically at a frequency of about 230 Hz. Also a spectrometer, a CCD camera, several photodiodes and a heater with temperature controller were parts of the laboratory set up.

- Demonstrator

Figure 3.13 shows a desktop demonstrator for integrated optical fluorescence sensing that has been designed and built recently. None of the measurements in this work has been performed using this compact module. It is optimized for performing all types of fluorescence measurements as well as the tests using electrochemiluminescence (ECL). A linear table allows automatic multiple pad or even multiple chip measurements, while the angular as well as the lateral adjustment has to be done manually. Modular construction allows different detection modalities; also a PM tube can be mounted to the demonstrator module. Two small lock-in amplifiers (Femto LIA-BVD-150-H) amplify the signal. The module can easily be transported and will be used in future by the Biochemical Sensors Section of CSEM in Neuchâtel.

3.3 Experimentel

- Assays

Most of the measurements have been performed using flow injection analysis (FIA) allowing switching between buffer, different sorts of sample solutions and regeneration fluids. A disadvantage of performing dynamic measurements in a micro fluidics flow cell is the quick generation of air bubbles and the not well-known flow distribution. Air bubbles adhere to the (chip-) surface. They therefore prevent the chemical reaction to take

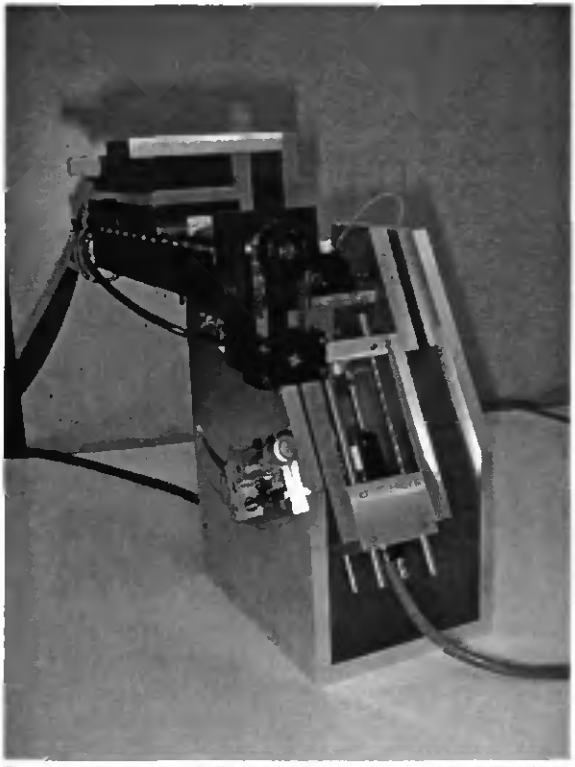

Figure 3.13: The new desktop sensing module incorporetes a laser that can be swung eround tha sensing region, e flow or still cell as chip holder, e scanning lineer table end read-out optics. A PMT can easily be connected.

place. Further they scatter the light enormously and thus meke the results unusable. The advantage of measuring in a closed flow cell is the possibility of arranging the sensor chip vertically. This point improves laser safety by means of a horizontal laser beam that is not coincidentally led directly or by reflection into the eye of the operator. This arrangement

furthermore offers en easier way to adjust the sensing pad on the center of the turntable. Adjusting the laser point on the sensing pad therefore is very easily performed. Further the flow injection option lead to the possibility of measuring the signal during the whole reaction process, which led to more meaningful results.

Some rare experiments were performed statically by filling the flow cell or putting some fluid containing analyte on the sensor chip using a pipette after turning the set-up into a position providing that the chip be horizontally lined up.

3.4 Fluorescent Dyes

Some different types of dyes have been tested for the measurements performed within this work. Cy-5 was the one used for all the relevant experiments. This label is very convenient as many molecules labeled with Cy-5 are commercially available. Additionally the measurements would not have been very reproducible if the set up had been changed too often when using differently colored dyes such as changing expensive optical filters and the angular settings. So most of the chips fabricated and used were optimized concerning the coupling angles for molecules labeled with Cy-5.

- Cy-5® - Dye

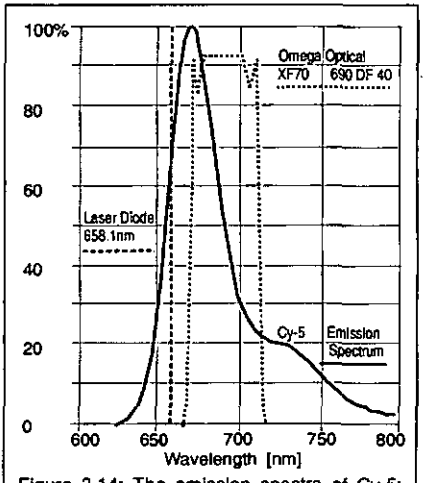

Figure 3.14: The emission spectra of Cy-5: peak wevelength at 670nm, mean around 690nm. Excitation maximum wavelength is eround 660nm.

Molecules labeled with the Cy-5 dye are available from Amersham Life Science. Besides the availability the Cy-5 dye is stable and its properties are well known. It is based on the benefits of cyanine flours and its emission band is comparably narrow.
Cy-5 offers high sensitivity; high sensitivity; low non-specific binding (if the labeling is strong); high photo stability; high water solubility and nearly pH insensitivity.
The absorption maximum is in the fer red at 649nm. The fluorescence ranges from 625nm to 800nm. Its maximum is at 670nm; the half-width totals 38nm, from 654nm to 692nm, thus the upper tail showing e smaller slope than the lower one (see figure 3.14).

- Cardio green

Indocyanine green (cardio green or fox green, Fluka, $C_{43}H_{47}N_2NaO_6S_2$, $\lambda_{ex} \approx 700nm$, $\lambda_{em} \approx 775nm$) was used for the very first preliminary feasibility tests using new replicated PC chips. It was not used for real experiments as its cost, lack of stability end limited absorbance in the visible region practically preclude it as a biological stain. Cy-5 is more convenient and offered excitation and emission wavelength very suitable for our chips.

- Ruthenium Complexes

For the singular series of electrochemiluminescence (ECL) measurements a ruthenium complex Ru(bpy) was used. See chapter 8.

- Absorption

Some tests with chips coated with an absorbing layer (mixture of ETH-5418 and KTTFPB) from Caspar Demuth from the Center of Chemical Sensors (CCS, part of the Swiss Federal Institute of Technology, ETH) have been performed thus showing too strong absorbance for our measurement set up and therefore a too high noise level.

4. Model Experiments

The feasibility of the new sensing schemes was tested in the measurement set up by performing different sorts of standard experiments. These well-known measurements of fluorescent molecules adsorbed to the chip surface were performed to show the behavior and the sensitivity of the new sensing schemes [39,40,44,51,56,60]. In these experiments a recognition layer was built on one sensing region by incubation of proteins during two hours. This built the sensing channel (S). In first experiments, only one sensing unit has been used on each chip for feasibility demonstration. Sometimes a second region was measured at the same time as a reference channel (R). This region was left clear or a blocking layer of bovine serum albumin (BSA) was incubated on it.

4.1 Immunoassays

- Protein A - IgG

One type of a model immunoassay was performed by incubating protein A onto one measuring pad to set up a strong and non-specific recognition layer for different types of antibodies (Jackson Immunoresearch Laboratories, Inc.). Incubation of bovine serum albumin (BSA) built up the reference channel, where no antibodies were expected to stay near the chip surface. Not all measurements however were performed on two (or more) channels.

The experiments consisted of an assay where a cycle with buffer solution (phosphate buffer saline, PBS) first was applied to calibrate the background baseline. Sample solution containing different concentrations of Cy-5 labeled entibodies (Goat-anti-Rabbit IgG; Donkey-anti-Mouse IgG) that stick to the protein A was applied in the next cycle. After the adsorption process saturated, buffer was applied again to show the net signal of labeled antibodies adsorbed to the protein A coated sensing layer on the chip surface. The signal from the reference channel during the application of the analyte containing sample showed the efficiency of background suppression by efficient coupling of the evanescent field. The net signal of that channel when it was again rinsed with buffer showed the effect of unwanted non-specific adsorption of labeled molecules to the chip surface.

- IgG - Antibody

For the other type of standard experimental immunoassays, mouse IgG molecules have been immobilized on a specific region of the waveguide-grating surfece of the chip using photobonding. The specified region - one single pad - represents the whole selective sensing unit. A sample solution based on phosphate buffered saline (PBS) containing 10nM Cy-5-conjugated donkey anti-mouse IgG as analyte was applied by means of a flow cell during several minutes in each essay. The reference channel was incubated with either BSA or another type of IgG was immobilized in

order to demonstrate the sensing scheme's multi channel measurement feasibility.
In the second case two grating regions of 1 mm x 1.5 mm each have been coated with two different IgG molecule types. These two regions were each working as independent single-pad sensing units (see inset in figure 4.5). One pad (1) was coated with mouse IgG whereas rabbit IgG molecules have been linked to the other pad (2). By applying a not recognized type of antibody each sensing unit worked exactly as a reference channel coated with a blocking layer does.

The experiments consisted of an assay where a cycle with buffer solution (phosphate buffer saline, PBS) first was applied to calibrate the background baseline. Sample solution containing Cy-5 labeled antibodies of one type (Goat-anti-Rabbit IgG) that stick to the Rabbit IgG was applied in the next cycle. After the adsorption process had saturated, buffer was applied again in a short cycle to show the net signal of labeled antibodies adsorbed to the Rabbit IgG coated sensing layer on the surface of one sensing pad. The signal from the other sensing channel during the application of the analyte containing sample showed the efficiency of background suppression by efficient coupling of the evanescent field like a usual reference channel as well as the specificity of the detection. The net signal of that channel when it was rinsed with buffer showed the effect of unwanted non-specific adsorption of labeled Goat-anti-Rabbit IgG molecules to the Mouse IgG coated surface of that pad. In a next step sample solution containing Cy-5 labeled antibodies of a different type (Donkey-anti-Mouse IgG) that stick to the Mouse IgG was applied. After the adsorption process on the Mouse IgG coated sensing pad had saturated, buffer was applied again to show the net signal of labeled antibodies adsorbed to the Mouse IgG coated sensing layer on the surface of the corresponding sensing pad. The other pad still showed the signal of the antibodies adsorbed during the first cycle. Hence that one could be considered as a reference channel in this cycle. Applying buffer during a long period showed the stability of the adsorbed molecules. A slow decrease of the fluorescence signal can give some information on the photo bleaching of the Cy-5 labels or wash out and different aging processes of the antibodies.

4.2 Results

- Protein A - IgG

The adsorption to the protein A coated pad can be observed dynamically to saturetion. Higher concentrations cause bulk fluorescence background on both channels. Also non-specific binding of molecules to the reference pad can be observed at higher concentrations. The net signal originating from the labels of the adsorbed antibodies can be obtained from the difference of the both final signals in buffer solution.

The curves in figures 4.1 to 4.3 show the increase of the emitted fluorescence intensity during the adsorption phase of the molecules to the

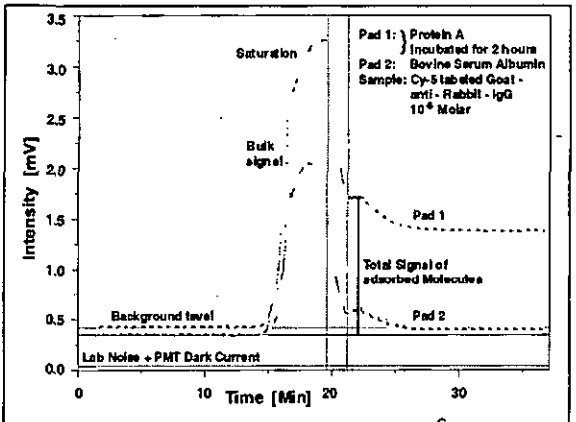

Figura 4.1: Standard experiment adsorbing 10^{-6} molar Cy-5 labeled goat-anti-rabbit IgG to an incubated layer of protein A. The bulk fluorescence contributes a high intensity.

sensing layer up to saturation. Each curve is a result of a measurement using another concentration of labeled antibodies. High concentration leads to a strong background intensity of light emitted by molecules in the bulk within the volume of the flow cell away from the chip surface.

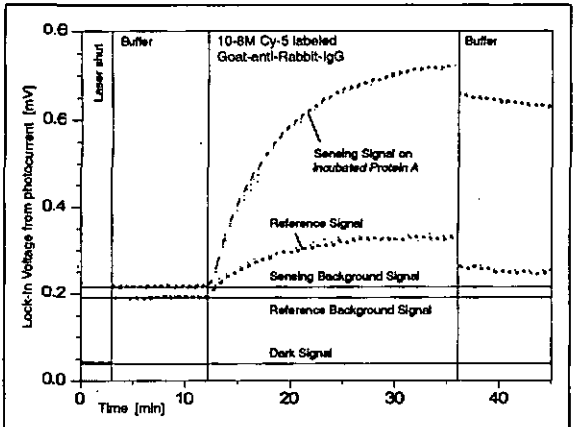

Figure 4.2: Standard experimant adsorbing 10^{-8} molar Cy-5 labeled goat-anti-rabbit IgG to an incubated layer of protein A. The bulk fluorescence contributes little intensity. Some unspecific binding seems to hava takan placa.

The background intensity originated from scattered excitation light, bulk fluorescence light, and polycarbonate fluorescence. Additionally, there is a small contribution by the PMT's thermal dark current (80cps @ 20°C).

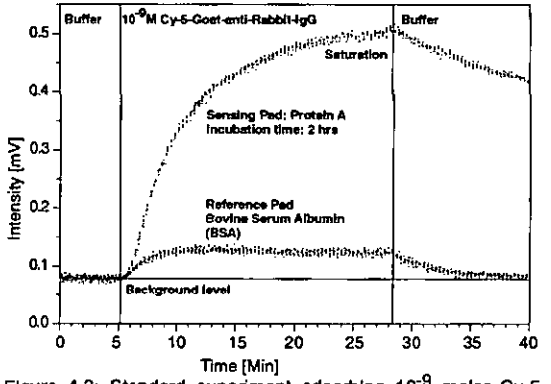

Figure 4.3: Standard experiment edsorbing 10^{-9} molar Cy-5 labeled goat-anti-rabbit IgG to an incubated layer of protein A. The bulk fluorescence contributes a small intensity.

- IgG - Antibody

The curve in figure 4.4 shows the increase of the emitted fluorescence intensity during the adsorption phase of the antibodies to the sensing layer of the corresponding type up to saturation. The isolated measuring points result from the repeatedly shut beam in order to reduce photo bleaching. The beam shutter has been opened for five seconds every minute.

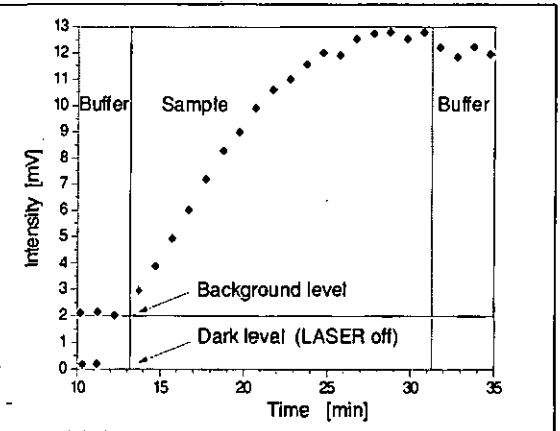

Figure 4.4: Adsorption phase of Cy-5 labeled goat anti-rabbit IgG on rabbit IgG.

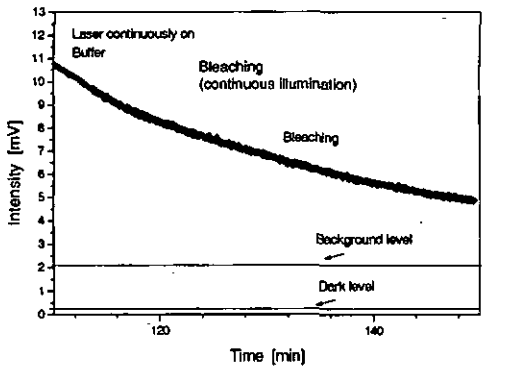

Figure 4.5: Photobleaching of the fluorescent dye due to continuous illumination after the experiment of fig.4.4.

As can be seen in figure 4.5, continuous illumination produces a much faster bleaching of the dye.

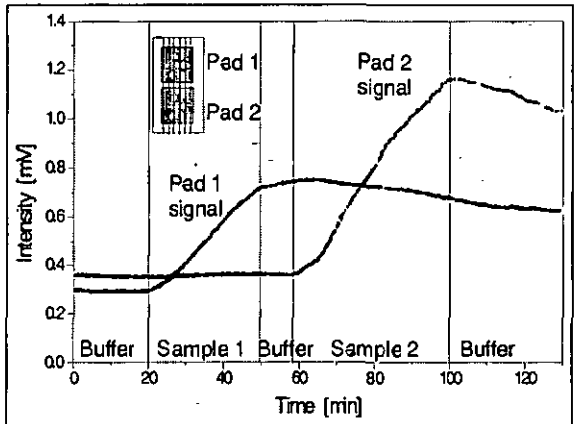

Figure 4.6: Fluorescence signal for a chip containing two sensing units. Neither unspecific binding nor bulk fluorescence can be observed.

Figure 4.6 shows the result of a two-channel assay. During the first cycle of the assay (time<60min) the sample only contained antibodies of one IgG type (10nM Cy-5 conjugated donkey anti-mouse IgG). Pad 1 shows the adsorption kinetics as expected. The second sensing unit on the sensor chip showed no response. It therefore could be used as a reference proving the absence of bulk signal.

After saturation of the first pad, antibodies of the second IgG type (10 nM Cy-5 conjugated goat anti-rabbit IgG) have been applied to the sensor. During this cycle, the analyte molecules adsorbed only on the second pad, while the first sensing unit served as a reference. The slight decrease of its fluorescence signal resulted from photobleaching.

The adsorption process of each pad can clearly be seen in the independent intensity raise of each channel. Only the corresponding antibodies are recognized and thus contribute to each signal. Each channel can be considered as a reference for unwanted effects such as temperature effects, non-specific binding, bulk background, aging of the labels, change of the coupling angle caused by pH changes or air bubbles in the flow cell by applying the antibodies of the type that does not correspond to the coating.

4.3 Discussion

The suitability of the approach has been demonstrated by performing standard immunoassays with replicated TiO_2 waveguide chips as well as with new glass based Ta_2O_5 waveguide chips, where an efficient discrimination between excitation light and fluorescent radiation was achieved. An excellent suppression of the unspecific contribution to the signal by the molecules in the bulk solution was also demonstrated. These standard experiments therefore give a good estimation of the label concentration limit needed for clear signals as well as about the efficiency of coupling end of background suppression in relation to the concentration. However they show that the time needed by the recognition and the binding process depends on the concentration to be measured. It is a fact that the saturation time increases exponentially with decreasing concentration. It can also be seen from the total of graphs that quantifying concentrations depends on very many factors that must be absolutely reproducible from chip to chip as well as from measurement to measurement. This point is the major problem to solve before quality sensors based on that principle can be produced.

- Protein A - IgG

The results show the adsorption of the labeled antibodies to the surface and the resulting fluorescence efficiently collected in the waveguide and coupled out to the detector. The advantage of the integrated optical method can be seen at low concentrations when the bulk fluorescence is strongly suppressed. In high concentrations the molecules present in the bulk contribute a high intensity of fluorescence making calibration extremely difficult as it is very difficult to quantify the percentages of emitted fluorescence intensity distributed to the different optical channels as stray light, guided modes to all directions, loss through the not observed TM angle, coupled at higher orders and even quenching effects. Photo bleaching and aging of the molecules on the surface can also be

observed. Whereas it is not clear what part of signal loss is due to bleaching, washing or different types of aging.

- IgG - Antibody

The results of the double channel standard immunoassay clearly show the possibility to perform multi-analyte sensing if stable recognition layers are coated onto the chip surface providing high specificity in their immunoreactions. Both pads do not show any unspecific edsorbing. Further the background suppression at a label concentration of 10^{-8} molar can be considered absolute. The channel sensing the antibodies in the first cycle (Goat-anti-Rabbit IgG) has complete reference channel properties. No relative change can be seen, as the other type of antibody does not bind to the antibodies of the first type already present on the surface. The antibodies of the wrong kind do not recognize binding sites that possibly remained free either. The constant intensity measured at that channel shows that the raise of the other signal must originate only from the binding process. This leads to the observation that the signal of the second antibody (Donkey-anti-Mouse IgG) is higher by nearly a factor 2. This effect cannot easily be understood. It might be an effect of a difference in the density of binding sites on the two different pads. Additional reference pads must be considered for real multi channel measurements. This fact is one of the problems to face if exact calibration for quantitative measurements needs to be performed. The structure of the recognition layer and its binding sites is one of the major key points in quantifying intensity measurements.
At this combination of molecules pure reference pads can be neglected. However that was not always the case. In performing multi-analyte sensing the combinations of molecules to detect have to be considered as carefully as the stability of each recognition layer.

5. Fluorescence-based Weveguide Detection of Antibiotics

After having shown the suitability of the new principle of sensing fluorescent molecules with the approach presented, the interest focused on detecting molecules of interest for a real sensor [7]. A current European project [74] focused on detecting antibiotic molecules in raw milk for food quality control using and comparing different sensing methods. So the same assays were used to show the feasibility of this approach in performing food control. In this chapter the detection of antibiotics is described.

5.1 Experimental

The method used to detect antibiotics was performing competitive assays. A competitive assay means here that a known concentration of antibodies (anti-PS) binding to e different type of antibodies (anti-mouse-IgG) with fluorescent dye labels (Cy-5) is added to the fluid to be analyzed. The labeled antibodies can either bind to the analyte molecules (antibiotics) or bind to one of the additional antibodies (anti-PS) in the fluid. This means

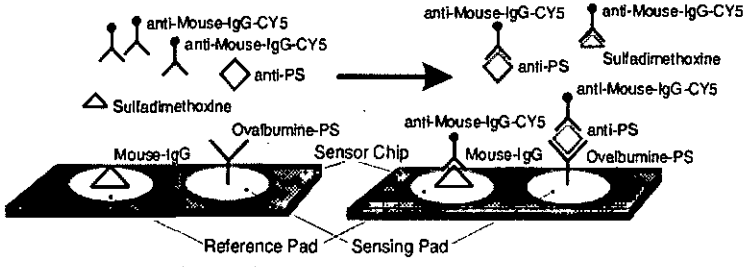

Figure 5.1: The scheme of a competitive assay for the detection of antibiotics (sulfamethoxina) in the fluid by measuring the amount of Cy-5 labeled anti-mouse IgG molecules captured by anti-PS molecules that adsorb to tha Ovalbumine-PS layer on to the sensor surface.

that the entibiotics and the extra antibodies compete for binding a lebeled antibody. The antigen recognition layer coated onto the sensing chip's surface (Ovalbumine-PS) only adsorbs those additional (anti-PS) antibodies (See Fig. 5.1). Therefore the intensity of the fluorescence signal on the sensor surface is decreasing if a high concentration of entibiotics is present in the sample, as the labeled antibodies captured by the antibiotics are not able to adsorb to the layer via the anti-PS and are washed away. As antibiotics are small molecules end have a big impact on organisms though appearing at very low concentrations, sensitive detection methods such as integrated optical fluorescence sensing are needed. Antibiotics can be found in blood as well as in a multitude of liquids of the food chain. For example the highly sensitive detection of the presence of antibiotics in milk and their concentration is a very important topic. For that reason many different experiments have been performed to detect antibiotics within this work.

5.2 Results

In a first assay sample solution containing both anti-PS molecules and Cy-5-labeled anti-Mouse IgG but no antibiotics, thus leading to a high fluorescence signal, was applied to a sensor chip coated with ovalbumine-PS (a derivative of sulfadimethoxine antibiotics) on the sensing pad, while mouse IgG had been coated onto the reference pad. The results shown in figure 5.2 show clearly that the signal of the sensing pad is higher then the signal of the reference channel although both pads are able to bind the mouse IgG, the sensing pad via the anti-PS whereas the reference pad binds them directly. This might be caused by the fact that the labeled antibodies bind to the anti-PS molecules in the solution already. This combination only can adsorb to the ovalbumine-PS coated sensing pad whereas solely the free anti-Mouse IgG bind to the mouse-IgG coated reference pad.

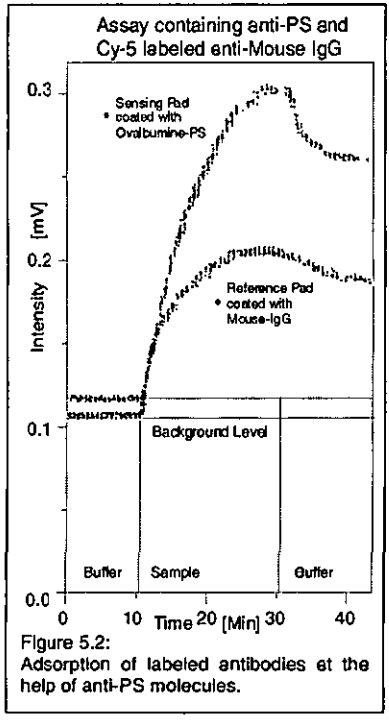

Figure 5.2:
Adsorption of labeled antibodies at the help of anti-PS molecules.

Figure 5.3 shows results of the detection of antibiotics using the same dual channel single pad scheme. On the sensing pad ovalbumine-PS has been immobilized by photobonding. The reference pad can be considered as a control channel and was coated with mouse IgG prior to the measurement. The sample solutions contained different concentrations of sulfedimethoxine and a fixed concentration of anti-PS as well as Cy-5 labeled anti-mouse IgG. This results in adsorption of the labeled anti mouse IgG molecules on the sensing as well as on the reference pad.
Both signals are presented versus time when flows of sample with different concentrations of antibiotic are passed through the fluidic cell.

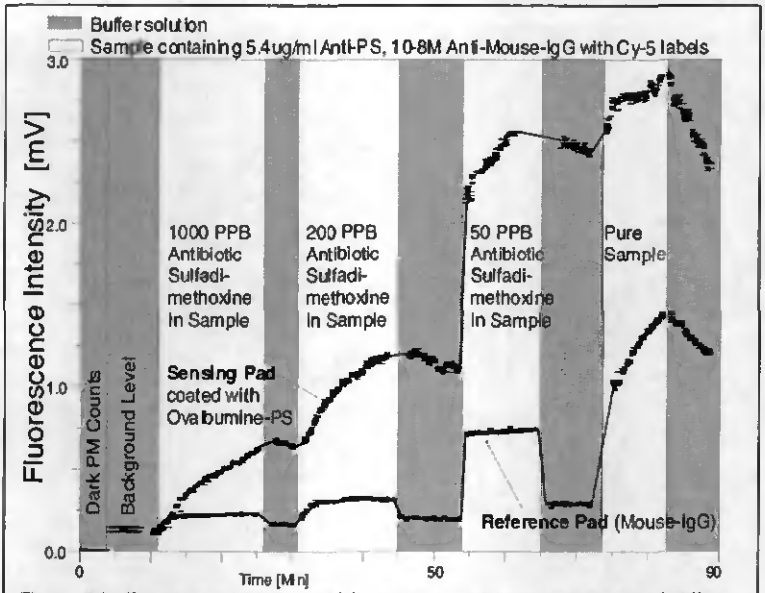

Figure 5.3: Experimental high-sensitivity sensor module measurement of different antibiotics concentrations. The rise of the reference signal is caused by the adsorption of anti-mouse IgG to the reference pad, which is not saturated.

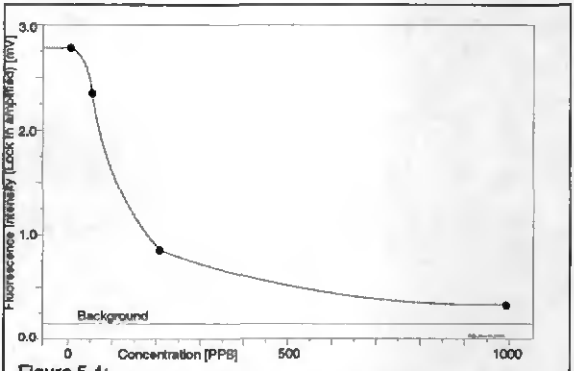

Figure 5.4:
Fluorescence measurement of a competitive essay using PS vs. Cy-5-lebeled anti-mouse-IgG in the presence of different concentrations of antibiotics. Measured after 3 minutes each.

Figure 5.4 shows the decrease of adsorbed anti-mouse-IgG-anti-PS fluorescence intensity as the concentration of antibiotics (sulfadimethoxine) in the sample solution is increased. This kind of curve can be used for calibration, as soon as the measurements will be standardized in order to get the highest possible reproducibility. Figure 5.4 however is not a calibration curve! It was gained from only one measurement, as the absolute signals between different measurements varied markedly. The most common result from all measurements performed was the observation that the reference pad coated with mouse IgG did not react independently from the presence of anti-PS and antibiotics. This fact was unexpected and is not understood.

Anyway, this experiment clearly demonstrates the increase of the fluorescent signal if the concentration of antibiotics diluted in the anti-PS solution is eventually decreased. The signal of the reference pad coated with mouse-IgG however was smaller than expected, as the adsorption of Cy-5 labeled anti-mouse IgG should not be influenced as anti-PS or antibiotics are present.

A different experiment is shown in figure 5.5. In the first cycle of the assay 10^{-7}M Cy-5 labeled anti-Mouse-IgG was supplied on the chip coated with one sensing pad of ovalbumine-PS and a reference pad of mouse-IgG. The labeled antibodies are adsorbed to the mouse-IgG pad. But the signal shows how they also stick nonspecifically to the ovalbumine-PS pad as the signal clearly increases. After saturation, anti-PS without labeled anti-mouse IgG was applied that caused both channels' intensities to decrease. The reference pad provided a clear net signal, whereas the sensing pad signal nearly extinguished. Supposedly it should have totally extinguished. The reference pad signal decreases slowly – be it from washing effects or – slightly, but not only – from photobleaching, or even from a different chemical reaction aging the molecules that was possibly caused by the anti-PS.

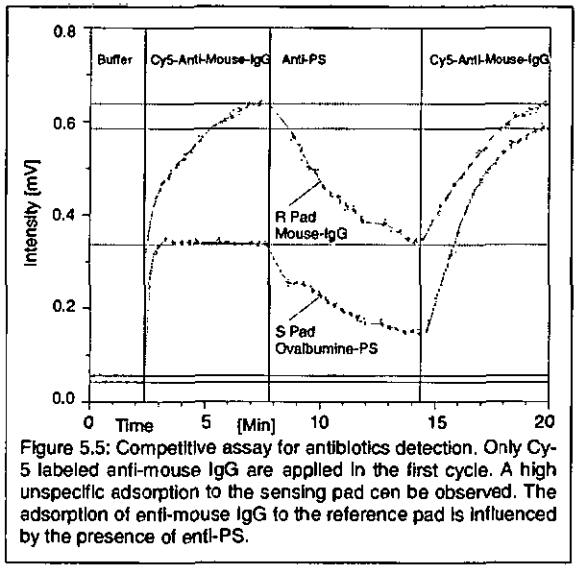

Figure 5.5: Competitive assay for antibiotics detection. Only Cy-5 labeled anti-mouse IgG are applied in the first cycle. A high unspecific adsorption to the sensing pad can be observed. The adsorption of anti-mouse IgG to the reference pad is influenced by the presence of anti-PS.

A similar experiment as the one described above lead to the result to ba seen in figure 5.6. In tha first cycle sample solution only containing labeled antibodies was pumped to the sensor chip. As in the experiment in figure 5.5 non-specific binding to the sensing pad could be observed. Then anti-PS molecules without fluorescent dyes were supplied. But the sensing pad signal rises as if tha anti-PS molecules did pick up Cy-5 labeled anti-

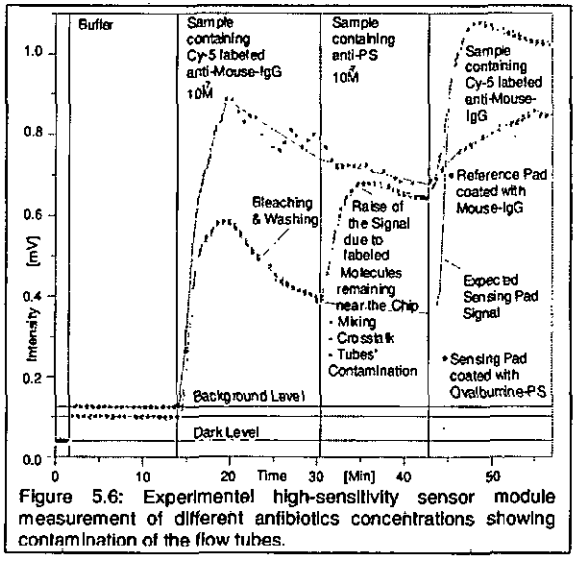

Figure 5.6: Experimentel high-sensitivity sensor module measurement of different antibiotics concentrations showing contamination of the flow tubes.

mouse-IgG through the contaminated tubes and now adsorb to the ovalbumine-PS pad obviously containing free binding sites. The anti-PS already carry the label with the anti-mouse-IgG.

In the third cycle labeled anti-mouse-IgG was supplied again as in the first one. Now the signal level of the reference pad increases again to a level similar to the first cycle one whereas the sensing pad signal rises to nearly the double intensity than before resulting from the adsorption of the labeled antibodies to every free anti-PS binding site.

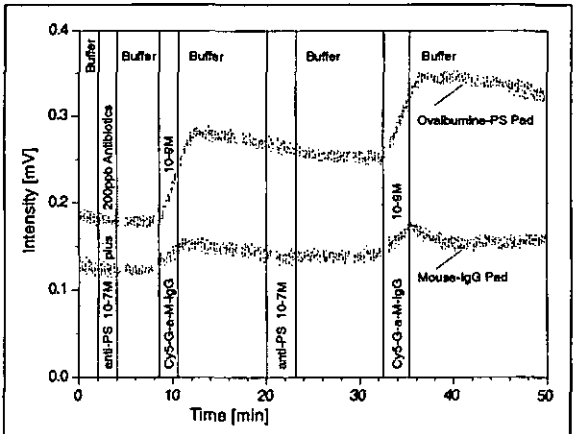

Figure 5.7: Competitive assay for antibiotics detection using anti-PS and a high concantration of antibiotics first, then applying sample containing analyte with fluorescent labels. Repeating this application with anti-PS but without antibiotics shows a signal increase.

The opposing assay led to the experiment that is shown in Figure 5.7. The assay began with the application of antibiotics and antibodies (anti-PS molecules) without eny labeled antibodies, as supposed not leading to any signal. After that Cy-5-labeled anti-Mouse IgG were applied leading to a rise in signal on both pads, whereas the intensity originating from the sensing pad was significantly lower than the one measured at the sensing pad. After a cycle of rinsing with buffer, a sample containing pure anti-PS but no antibiotics was applied. This did not cause an intensity change again. When finally labeled antibodies were pumped through the flowcell again, the signal measured at the sensing pad again increased. The intensity measured through the reference channel did not change greatly, hence a significant instability can be observed.

5.3 Discussion

The suitability of the approach to detect antibiotics using competitive assays has been demonstrated by performing different types of antibiotic immunoassays with replicated TiO_2 waveguide chips as well as with new glass based Ta_2O_5 waveguide chips. An efficient discrimination between excitation light and fluorescent radiation was achieved. However some effects were not absolutely understood. The possibility of cross talk between the sensing units, tube contamination by dye molecules, unstable recognition layers and other problems seem to be some explanations for unexpected signal variations. Even examining the chips in an ArreyScanner after use did not help finding definite answers for these signal variations.

The new detection scheme was nevertheless successfully demonstrated and the compatibility with a fluidic cell indicates that it is possible to expand the range of applications by integrating the whole system into a compact module for performing measurements at the point of demand.

- Applications
  - Immunoassays for diagnostics on the ppb level
  - Assays for sensing of small molecules
  - Exemples:
    - Antibiotics in milk
    - Drugs in food or blood
    - Wastewater enalysis

6. Detection of Oligonucleotide Tailing

In this section the detection of DNA probes using the single-pad waveguide fluorescence sensing method will be described. The interest in detecting DNA probes [1,2,3] is still growing, as it leads to an understanding of many different kinds of inherited diseases. A main goal is to apply this understanding into faster and more accurate techniques for diagnosis and treatment [11,20,51,55,59,60].
Therefore, experiments have been performed using a new assay measuring oligonucleotides labeled with fluorescent dyes that were adsorbed to the single pad IO sensor surface by a forced tailing reaction for fluorescence signal amplification (Figure 6.1). Tailing means that multiple DNA target probes (oligonucleotides such as d-ATP and d-CTP) adsorb specifically to one binding site immobilized on the chip (primer)

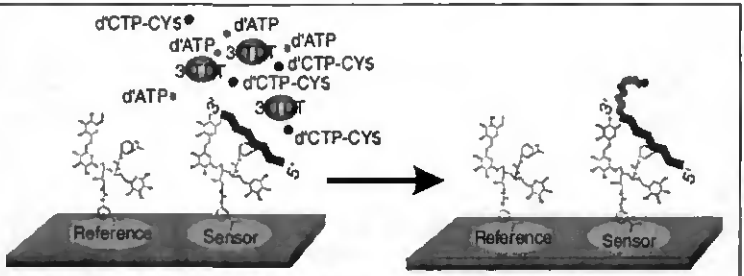

Figure 6.1: The scheme of the tailing reaction on the sensor surface.

building up a chain. In this assay, oligonucleotides were immobilized on the sensor surface by dextran-based photobonding and then hybridized with complementary oligonucleotides (analyte). The tailing reaction of the nucleotides was forced using 3'terminal deoxynucleotidyl transferase (3'TDT) as an enzyme [75].

6.1 Experimental

The 3'TDT reaction mixture contained fluorescent nucleotides; that are, Cy-5 labeled oligonucleotides. After a feasibility demonstration of the tailing reaction using the conventional IO sensing scheme described in chapter 2, a new series of experiments has been performed using the single-pad scheme of figure 2.1. The cycle started applying PBS buffer prior to OPA (one phor all) buffer. Then the tailing reaction of the oligonucleotides was forced by applying d-CTP, d-ATP and 3'TDT solved in OPA buffer. To measure the net signal, pure OPA buffer was applied again to finish the cycle.
The concentration of oligonucleotides was as follows:

d-ATP: $3 * 10^{16}$ units / 30 µl

Cy-5 labeled d-CTP: $1.5 * 10^{14}$ units / 30 µl

$3 * 10^{13}$ units / 30 µl

(Molecular weight ≈ 330 Daltons)

As the tailing reaction is very slow and strongly depends on the temperature and the enzyme concentration very long cycles have been performed. In order to get information on the tailing process despite the high bulk intensity during these long cycles, OPA buffer was intermittently supplied every few minutes.
Coupling angle of the PC chips were +52° (laser TM, in) and +64° (fluorescence TE, out).

6.2 Results

All measurements show the long time scale of the tailing reaction as well as enormously high bulk contribution that raised the signal nearly or fully out of range. Figure 6.2 and 6.3 each show such a tailing cycle performed on a TiO_2 waveguide on a PC chip and on a Ta_2O_5 waveguide on a glass chip (Artificial Sensing Instruments, ASI) respectively. The net signal after the reaction supposedly was stopped is the contribution of the nucleotides bound to the surface by the tailing reaction.

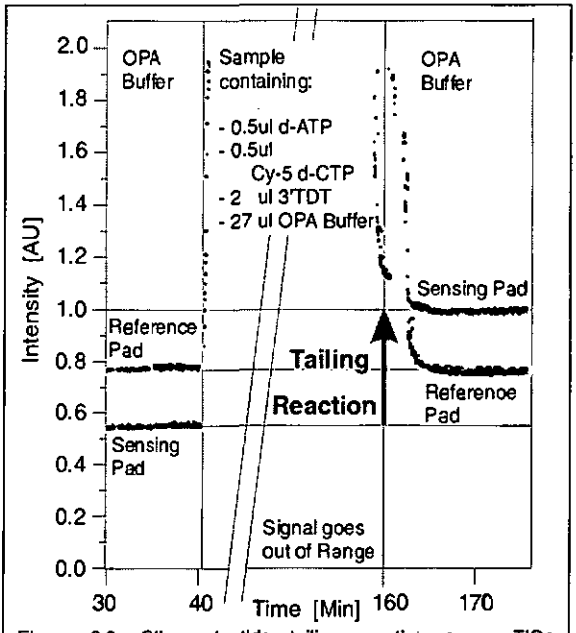

Figure 6.2: Oligonucleotide tailing reaction on a TiO_2 waveguide (replicated polycerbonate (PC) chip). A very high concentration of labeled oligonucleotides is present in the bulk volume. However the baseline is very stable; no drift or unspecific binding of oligonucleotides onto the T-Dextran surfece is obsarved.

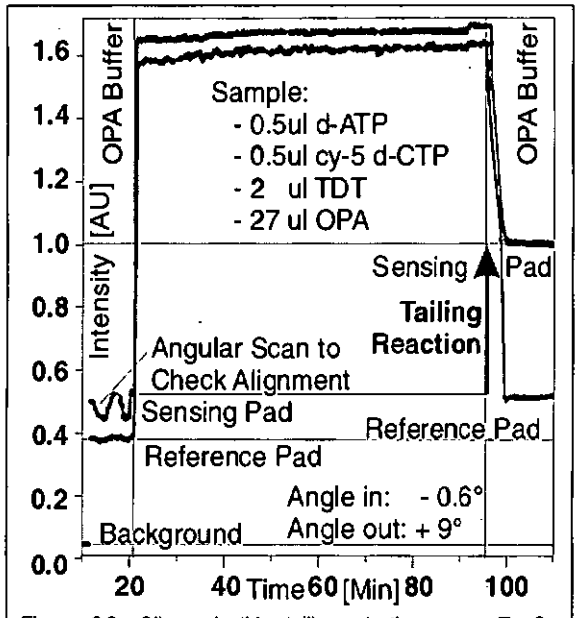

Figure 6.3: Oligonucleotide tailing reaction on a Ta_2O_5 waveguide (glass chip). A very high concentration of labeled oligonucleotides is present in the bulk volume. A slight drift in the baseline is observed.

Figure 6.4 shows results of an experiment where the same sample containing labeled oligonucleotides was used multiple times to initialize the tailing reaction as well as for its continuation. In order to selectively monitor the signal originating from the oligonucleotides immobilized to the chip surface, buffer solution was applied intermittently for washing away the fluorescent mononucleotides present in the bulk sample.

Figure 6.4 clearly shows the gradual increase of the "surface signal" produced solely by oligonucleotides at the very surface of the sensor chip as the tailing reaction proceeds. The adsorption took place in-situ during the cycles where the sample solution was applied to the flow cell (white regions in figure 6.4).
The decrease of the signal maximum of the bulk fluorescence results from the fact that the same sample volume has been reused for each cycle. So its oligonucleotide concentration and the amount deposited reversibly on the surface decreased in each cycle. In addition to that the dyes in the sample solution suffered – as well as the immobilized ones - from photo bleaching.
In summary, it has been demonstrated that the 3'-TDT tailing reaction on target oligonucleotides can be monitored and measured by fluorescence-based integrated optical single-pad sensing.

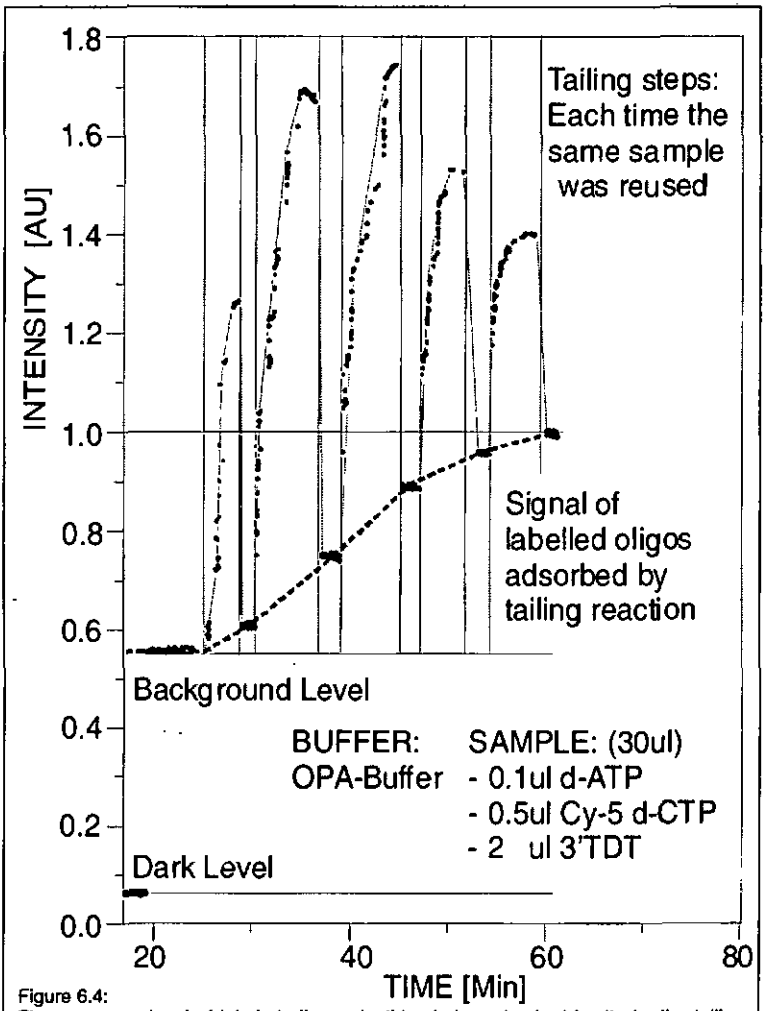

Figure 6.4:
Fluorescence signal of labeled oligonucleotides being adsorbed in-situ by the tailing reaction. The dynamics of the adsorption can be observed by eliminating the bulk.

6.3 Discussion

The detection of the oligonucleotide tailing reaction does not necessarily have to be performed with integrated optical sensing, as the concentration of analyte moleculas in the sample solution used for the reaction is high compared to the detection limit of this type of sensing. However, the

portion of labeled molecules was reduced compared to the total amount (1:4) of reactive molecules (oligonucleotides). Therefore each chain or tail of adsorbed oligonucleotides contained some particular Cy-5 labeled oligonucleotides that contributed enough fluorescence intensity to the total signal in order to measure at least qualitatively. The signal actually can be calibrated as a labeled oligonucleotide concentration of 20% can be assumed.
The results show that the concentration of labeled oligonucleotides was still high, as the background light resulting from the fluorescence labels in the fluid (bulk) could not be suppressed.

The cross-polarized portion of the light emitted by the dye-labels on the chip surface is coupled out of the waveguide via the same grating pad, but at a different angle. At this angle the emitted light signal was detected spatially separated from the illumination background.
The performance of this novel approach has been demonstrated using a single pad IO sensing scheme. The concentration of labeled oligonucleotides is rather high for the use of integrated optical sensing despite the fact that only 20% of the target probes were labeled. Still the results clearly show the efficient light collection by the waveguide.

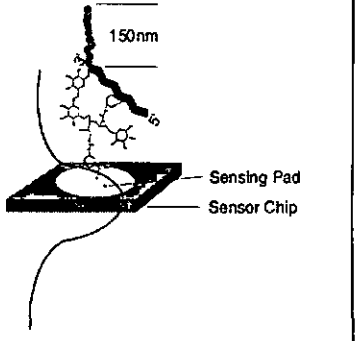

Figure 6.5: Long oligonucleotide tails get out of the evanescent field range.

A limiting factor however is the length of the oligonucleotide tails. If they get too long, the evanescent field of the guidad mode is too week to be influenced in either way of the light (illumination as well as emission). Having an average diameter of 15.4nm [76] and respecting the thickness of the recognition layer, the labels get out of the efficient range of the evanescent field from chains longer than about 10 oligonucleotides (Figure 6.5).

The penetration depth of the evanescent field is calculated by:

$$\Delta x_{fs}^{(s,p)} = [\lambda/2*\pi*((N^2-n_s^2)^{1/2})]*[n_f^2/q_{fs}*\varepsilon_{es}+N^2)]^p \qquad (6.3.1)$$

with: $\varepsilon_{es} = N^2 - n_s^2$ $\qquad$ $q_{fs} = n_f^2 / n_s^2$

7. Detection of Oligonucleotides with on-Chip Hybridization

Experiments of a different type have been performed detecting poly-A_{30} oligonucleotides. The poly-A molecules are single stranded 30-mer oligonucleotides that have got a hairpin loop of adenosines on top of a specific DNA sequence, as schematically shown in figure 7.1. Poly-A_{30} molecules are polydeoxyadenosines with a loop length (L) of 30 adenosines. These oligonucleotides adsorbed to a Dextran based DNA recognition layer that was immobilized on the surface of the sensing ped by photobonding. This leads to a specific binding reaction of a single poly-A_{30} molecule to each binding site (not comparable to the tailing reaction described in chapter 6). The DNA-probes (oligonucleotides) are denatured at the temperature T_m = 47.8°C [77].

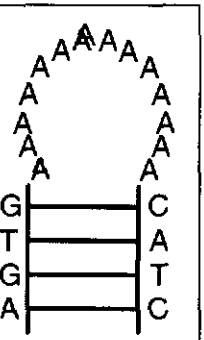

Figure 7.1: Scheme of the polyadenosine$_{30}$ (poly-A_{30}) molecule: 30 adanosines build a loop on top of a DNA sequence.

The idea was to heat the chip during the experiments to dehybidize the molecules hence regenerating the chip for new experimental cycles [7,55,59].
At temperatures higher than T_m the molecules start to dissociate from the chip surface. Therefore the heating was pushed up to 82°C. To then hybridize the surface again the chip was rinsed with Tris-HCl buffer.

7.1 Experimental

The sample solution used contained 50ng/ml Cy-5 labeled poly-A_{30} (molecular weight = 10.416 Dalton), which corresponds to a $5*10^{-6}$ molar concentration. A reference solution containing the same concentration of Cy-5 labeled polydeoxycytosine (poly-C_{30}) instead of poly-A_{30} is used to check the signal background. Actually no rise could be observed by applying this reference solution. Therefore the supply of poly-C_{30} did not ceuse bulk background even. It must be assumed that the poly-C_30 molecules stay quite far away of the dextran-based recognition layer. After the adsorption (shown in figure 7.2) to the integrated optical single pad fluorescence sensor chip and a rinsing phase with 2xSSPE buffer the molecules were dehybridized by heating the flow cell to 82°Celsius. Re-hybridization was performed on-chip rinsing the active sites with Tris-HCl buffer. After this regeneration of the chip and a long washing phese with again 2xSSPE buffer (SSPE Buffer, pH 7.4, A NaCl/Phosphate/EDTA buffer (10mM Tris HCl, 0.1mM EDTA) used in DNA wash and hybridization solutions) a new cycle of a Poly-A_{30} containing sample was performed to repeat the adsorption process. The signal can be seen to rise near the

maximum that was reached in the first essay. Therefore the properties of the Dextran-based recognition layer do not seem to suffer from the dehybridization process.

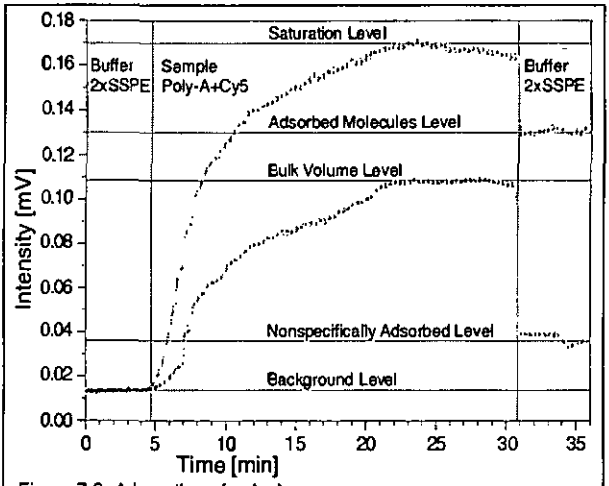

Figure 7.2: Adsorption of poly-A_{30}.

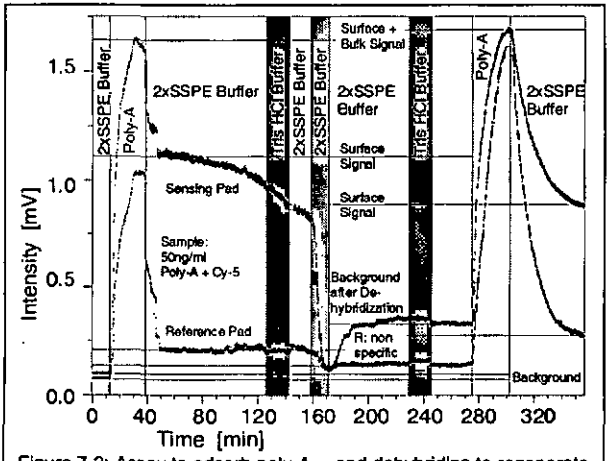

Figure 7.3: Assay to edsorb poly-A_{30} and dehybridize to regenerate the sensor chip by heating.

7.2 Results

The results show that mainly the poly-A_{30} which are bound specifically to the sensing pad on the chip contribute to the net fluorescence signal

detected via the evanescent field propagating in the waveguide. By heating the chip the dehybridization takes place very quickly (see figure 7.3). The signal loss after the molecules dissociate from the surface can be seen very clearly.

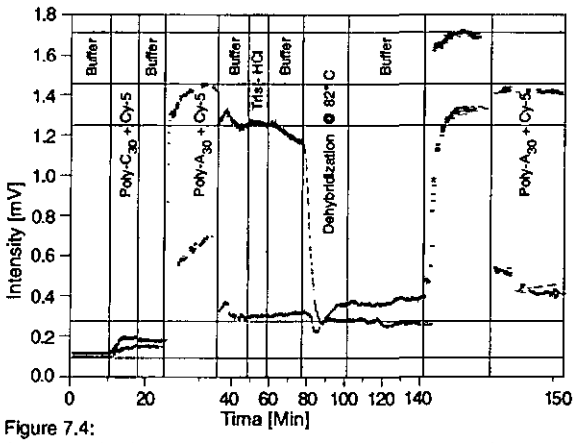

Figure 7.4:
Assay to adsorb poly-A_{30} end dehybridize to regenerete the sensor chip by heating. The time scale was nonlineerly stretched for better visualizetion of the adsorption dynamics.

A stretched detection signal curve (compressed dehybridization cycle) can be seen in figure 7.4). It shows the repeated adsorption process of labeled poly-A_{30} molecules to the sensing pad.

7.3 Discussion

As a concentration of $5*10^{-6}$M Cy-5 dye molecules is high for this kind of detection high bulk fluorescence can be observed as long as the sample is present in the flow cell. The reference solution however does not cause the same bulk intensity what can be caused by the possible fact that the poly-C_{30} molecules never go that close to the surface of neither pad.

The specific edsorption of the poly-A_{30} molecules to the sensing pad can be clearly seen. The reference pad coated with pure Dextran only showed the bulk background intensity. After applying buffer its signal decreased to the background level.

8. Tests of Combining IO with ECL

- Preliminary Tests of Deposition of a Ta-Pt Layer on Plastic Chips

Many different preliminary tests and very first measurements for using integrated optical sensing techniques to detect electrochemiluminescence (ECL) [70,71] have been performed. Theoretically the advantage of such a combination is the efficient collection of the luminescance light having a weak intensity into the waveguide and thus getting a better signal.

First of all platinum electrodes had to be applied onto an integrated optical sensor chip surface. For testing the feasibility of the electrode coating process a macroscopic layer of platinum has been applied to some IO PC chips. See Figure 8.1.

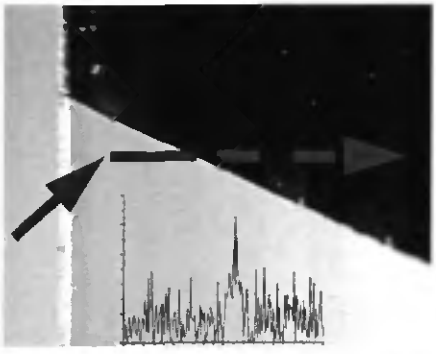

Figure 8.1: PC chip coated with a large Pt layer. Tests showed that the light is continuously propagated beneath the electrode. The included angular scan shows a coupling peak.

The layer was tight and homogeneous but the adhesion was insufficient and, mostly, when using a shadow mask for fine structures it has to be removed later using acetone and other aggressive solvents. This led to the understanding that PC chips could not be used for such applications. But the dielectric property of the chip could still be observed when light was coupled into the weveguide. Measuring the resonance in an angular scan at the edge of the chip where the light propagated beneath the metallic layer lead to clearly visible peak, which also is shown in figure 8.1.

- Electrode Design

When the CSEM-Unaxis glass chips became available another try was performed to deposit thin electrode bands onto the chip's wave guiding surface. Luca Berdondini of the IMT Neuchâtel was successful. Figure 8.2 shows the layout scheme of the chip and the Ta-Pt electrode bands to be coated. Electrode duty cycles of 10µm/10µm, 10µm/20µm and 25µm/25µm have been designed. The electrodes were fabricated by depositing a 150 nm Ta-Pt layer onto the glass chip surface that was pretreated using photolithography.

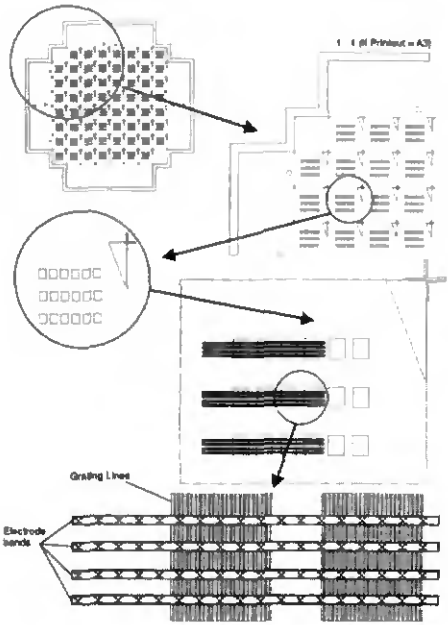

Figure 8.2: Mask design by Luca Berdondini for applying Pt electrode bands to a waver of 62 integreted optical glass chips.

The light should be generated near the edges of the electrode bands and propagate in the waveguide beneath. Then it should be coupled out via the grating at 8.4° (TM mode) and at 2.25° (TE mode).

Figure 8.3 shows a photograph of such a chip bearing thin electrode bands. To test the wave guiding properties of these chips they were illuminated. A He-Ne laser beam was directed onto a grating region to couple into the waveguide. Figure 8.4 shows that the light is propagated in the waveguide beneath the electrode bands both illuminating a non covered pad as well as illuminating an electrode-covered pad. This is not obvious as the metallic layer on the surface is supposed to change drastically the dielectric properties of the waveguide.

8.1 Experimentel

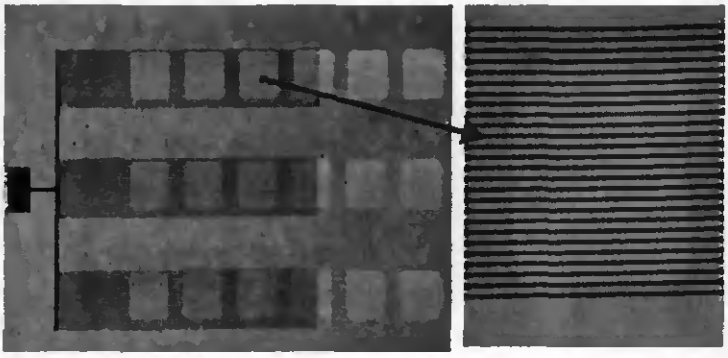

Figure 8.3:
Thin electrode bands have been deposited onto the wave guiding film on a glass chip.

For testing the feasibility of real ECL measurements it was considered to put an electrochemiluminescence active Ruthenium complex solution into a still cell with the chip bearing electrode bands mounted. Then an electric potential was applied to the electrodes using a potentiostat. The generated ECL should be directed efficiently to the detection optics and the PMT via the grating. In order to see the order of magnitude of the efficient luminescence collection and coupling an angular scan from –12.5° to +12.5° was performed with the turntable whereas the PMT was fixed on its position.

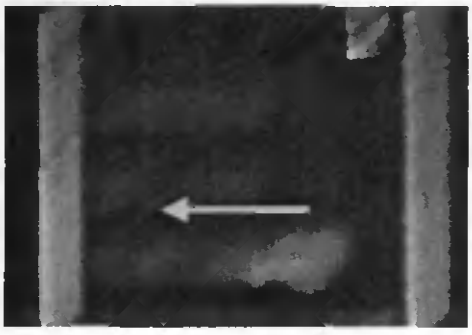

Figure 8.4: The light is coupled into the waveguide through an uncovered grating pad and propagates beneath the electrodes. Outcoupling can be seen at a grating pad covered by Pt bands.

8.2 Results

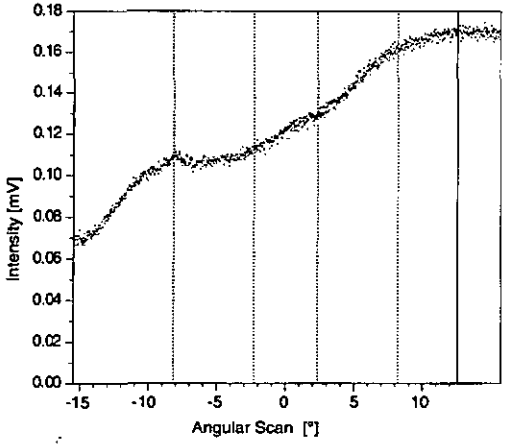

Figure 8.5: The intensity variation of the ECL signal during an angular scan of 18 minutes. A strong drift is visible.

Figure 8.5 shows the intensity during such an angular scan. It is obvious that the symmetry of peaks could not be observed. However, the maximum signal is not observed at 0°, as it would be expected if only the diffuse ECL signal was detected. The whole ECL intensity seems to drift during the angular scan that lasted 16 minutes. The intensity maximum at –8.3 degrees is thought to probably originate from efficient coupling. The result to be seen in figure 8.6 could possibly show a resonance too. As the spectre of the Ru(bpy) is very wide a large angular coupling region must be expected.

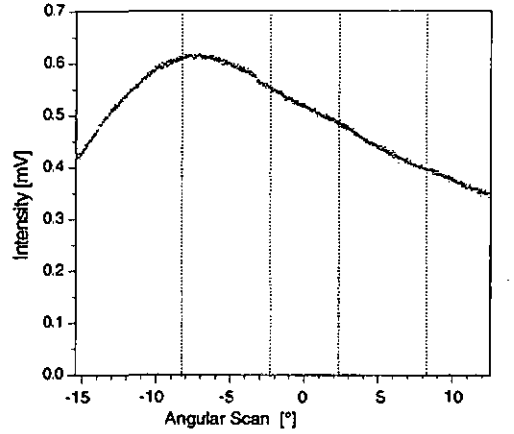

Figure 8.6: A clear intensity peak can be seen if the chip is rotated to one angular region from zero. Asymmetry may result from modes propagating in one direction only. The wideness is caused by the wide spectra of Ru(bpy)

8.3 Discussion

The only measurements that have been performed have not been very promising. The reasons for their failure are not obvious. Some points to be considered according to the observations:
There might have been too much light intensity for the luminescence was clearly visible by eye. Hence, the part of light having been guided through the waveguide and coupled out via the grating must have been comparably small and thus vanished within the noise. The portion of luminescence coupled into the waveguide and coupled out to the detector via the grating might only become efficient beyond the visible threshold.
Additionally we had the impression that the visible light was propagating in the waveguide parallel to the grating lines. This could be an effect of the fact that the electrode bands were placed rectangular to the gratings and had some kind of grating effect to the light. A fact to consider is that the metallic layer may influence the effective refractive index of the waveguide in a destructive way. It therefore hes to be thought of a new design of IO ECL sensor chips that have electrode bands between the grating pads being parallel to the grating lines.
Further no specific ruthenium ECL peak band pass filter has been used.
To detect the signal and suppress a little bit the background light a chopper was placed in front of the flow cell to modulate the luminescence and detect the voltage into which the photocurrent has been converted using a lock-in amplifier.
Further problems resulted from the very small volume of the used flow cell. As air bubbles develop from the counter electrode the volume was quite quickly displaced by air, which makes optical measurements nearly impossible. Sometimes the bubbles also disconnected the reference electrode from the fluid and therefore stopped the luminescence at all.
For ongoing measurements faster data transfer must be possible. The more measuring points can be recorded in time the faster are the angular scans.

9. Conclusions

Novel types of sensing schemes have been presented that are suitable for accomplishing single-chip array sensors based on fluorescence. Each element of the array represents an independent measuring channel with an individual bio coating immobilized on its surface. The presented work shows how these new schemes for fluorescence-based biochemical sensors have been designed, fabricated and used for different kinds of measurements. Many problems led to an optimization of the sensing principle while others could not be totally solved within the frame of this work. The new approach of detecting fluorescent labeled molecules on different kinds of integrated optical chips on single-pad sensing channels shows the possibility to get high density multi channel sensors with small and disposable integrated optical sensor chips providing enough space for different types of molecules on the same surface. It has been shown that all the tasks of light input, excitation of the analyte molecules, fluorescence light collection, and optical readout can be performed by means of a single grating coupler pad per channel. The results showed a low detection limit. This could be pushed further down for example by using a cooled PMT or performing photon counting. In the typical arrangement, TM-polarized light was used for exciting the molecules by direct illumination as well as by the evanescent field of the guided wave. In contrast to the conventional schemes, the fluorescence light was collected at the orthogonal polarization via coupling to the TE_0 waveguide mode [16,73]. Radiation emitted by the dye molecules present in the bulk medium is better suppressed by using evanescent waves not only for illumination, but also for collecting the radiation emitted by the molecules immediately adsorbed to the recognition layer. The advantage of collecting the light in the planar waveguide of an integrated optical chip due to the properties of fluorescence generated close to a surface of high optical density [36] to enter the waveguide was shown at very low concentrations.

Experiments have shown that this method can be used for the detection of different types of bio molecules such as DNA probes or antibiotics. But also drugs, hormones or heavy metals can be considered as to be detected using fluorescence-based integrated optical sensing. The advantage against refractometry becomes effective for small molecules.

Besides a good signal-to-noise ratio, an additional benefit is the small area needed per sensing channel, facilitating single-chip multi-channel sensing. Furthermore, it was also shown that it is possible to use replicated sensor chips based on plastic substrates [78].

Compared to the wide field of sensor development by many different research groups the highest sensitivity [7,31,58,59,60] could not be equalized, but ranges in the upper area. Still this approach is very promising since it provides a sensitivity high enough for many applications and it offers the possibility of fast high-density multi channel measurements on e simple set-up using comparably low-cost sensor chips. With respect to the late availebility of glass chips it was not possible to perform many of the modifications mentioned above for improving the sensor within the given time frame of this work.

In summary, this thesis has presented a new approach for detecting bio molecules with a small sensor set-up in a simple and low-cost way. The combination of integrated optical sensing with fluorescent labels leads to a high sensitivity, and the single pad scheme allows multi-channel measurements with high density. The results show the potential of this new approach to become a leading detection tool.

Method	Type of Detection	Measurand	Label	LOD	Reference	No.
Integrated Optics	Fluorescence	Proteins, DNA Probes	Cy-5	not determined	*Present Work*	-
				Signal at 10^(-10) M		
Integrated Optics	Fluorescence	Proteins (Antigens)	FITC	10^(-10) M	*M.Yoshida et al*	*23,41*
Integrated Optics	Fluorescence	Proteins	Cy-5, Fluorescein, ...	10^(-14) M	*T.E.Plowman; D.Christensen et al*	*50*
Integrated Optics	Fluorescence	DNA Probes	Cy-5, Fluorescein, ...	10^(-16) M	*W.Budach et al*	*55*
Integrated Optics	Fluorescence	Proteins (Antigens)	A-FITC	2.4^(-9) M	*Y.Zhou et al*	*52*
Integrated Optics	Fluorescence	Proteins	Cy-5, Fluorescein, ...	3*10^(-15) M	*G.L.Duveneck; T.E.Plowman et al*	*50,51*
Integrated Optics	Fluorescence & Electrochemistry	Proteins (Antigens)	FITC	10^(-7) M	*A.Asanov; P.Oldham et al*	*10,13*
Integrated Optics	Luminescence	Gangliosde Receptors	self Luminescence	1.5*10^(-6) M	*D. Kelly et al*	*34*
Integrated Optics	Extinction		methylen blue	10^(-4) M	*T. Okamoto et al*	*69*
Integrated Optics	Absorption	methylene blue	methylene blue	3*10^(-6) M	*T. Okamoto et al*	*69*
Integrated Optics	Interferometric	Proteins		10^(-10) M	*R.G.Heidemann et al*	*29*
Integrated Optics	Interferometric (Phase shift)			2*10^(-13) M	*Schlatter et al*	*30*
Integrated Optics	Interferometric (Phase shift)	Proteins (Antigens)		3*10^(-8) M	*B.J. Luff et al*	*28*
Integrated Optics	Refractometry	Proteins (Antigens)	free --> adsorbed mass	10^(-10) M	*M.Wiki et al*	*45*
Fiber Sensors	Integrated Optics	Proteins (Antigens)		10^(-7) M	*O.Wolfbeis et al*	*48*
Fiber Sensors	Integrated Optics, Fluorescence	Enzym: Creatine kinase	B-phycoerthrin	10^(-10) M	*I.M.Walczak et al*	*63*
Absorbance Spectroscopy	Spectroscopy	Amines	different	10^(-3) M	*G.Mohr et al*	*79*
Fluorescence	Fluorescence Polarization	Protease	5-aminofluorescein	5*10^(-10) M	*L.M.Levine et al*	*16*
Fluorescence	Directly Illuminated	Proteins	different	---	*ELISA*	*7*
Fluorescence	Lifetime	CO2 and others	Pt- and Ru-Complex	--- / 10^(-7) M	*O.Wolfbeis; Lakowicz et al*	*18*
Fluorescence Decay	Fluorescence Anisotropy	Anthracene	Anthracene	10^(-4) M	*M.E.Lippitsch*	*17*
Fluorescence Decay	Time Resolved	DNA Probes	Cy-3	10^(-7) M	*G.Valentini*	*20*
Electrochemiluminescence	ECL	Codeine / Glucose	Ru-Complex	10^(-4) M / 5*10^(-5) M	*E.L'Hostis et al*	*71*
Electrochemiluminescence	ECL	*pure label*	Ru-Complex	5*10^(-7) M	*G.C.Fiaccabrino*	*70*
Surface Plasmon Resonance	SPR	Proteins	free	10^(-11) M	*BIAcore*	*7*
ToF Mass Spectroscopy	Time of Flight	Proteins (Antigens)	free --> mass	throughput / crosstalk		*7*
Electrochemistry	Electrochemistry	digoxin		10^(-11) M	*Kaneki et al*	*5*
SNOM		Proteins (Antigens)	Any	single molecules	*R.Eckert et al*	*80*

CHEMICAL DATA

Anti – IgG Antibody
Antibodies used were all from Jackson Immunoresearch Laboratories Inc.

ARC Anti Reflection Coating
Brewer Science Inc.
Product: ARC XL-20
Thickness (spin coating at 3000 rpm, 168°C, 60 sec): 240 nm
Absorption at λ = 365 nm to 436 nm: 1.14 ± 0.06
Components: Cyclohexanone (50-65%), n-Methyl-2-pyrrolidone (30-40%), Polymer solids (1-10%), Dye solids (1-10%), Aluminum (67ppb), Calcium (26ppb), Copper (56ppb), Iron (210ppb), Potassium (15ppb), Sodium (<12ppb)

BSA Bovine Serum Albumin, Sigma

dATP 2'-deoxyadenosine 5'-triphosphate
Amersham Pharmacia Biotech

DNA Desoxyribonucleic acid

IgG Immunoglobulin G.
Antigen
Molecular weight: ~150'000 Dalton

OPA All phor one buffer
Pharmacia
Product: 27-0901-02
10mM Tris-acetate pH 7.5, 10mM magnesium acetate, 50mM potassium acetate

Poly-A Polyadenosines
DNA target probes

Ru(bpy) A redox-cycling ECL type ruthenium complex

Wevelengths of some fluorophores

Fluorophore	Excitation	Emission
5-Hydroxytryptamine (5-HT)	400 nm	530 nm
Acridinyellow	470 nm	550 nm
Acridinorange	470 nm	530-650 nm
Auramine	460 nm	550 nm
Aurophosphine	450 nm	580 nm
Berberbinsulfate	430 nm	550 nm
Bisaminophenyloxidiazole (BAO)	280 nm	460 nm
Catecholamine	410 nm	470 nm
Coryphosphine	460 nm	575 nm
Cy 3	546 nm	580 nm
Cy 5	649 nm	670 nm
Cy 5 TOTO 3 (DNA specific)	633 nm	670 nm
Euchrysine	430 nm	540 nm
Fluoresceinisothiocyanate (FITC)	490 nm	525 nm
isothiocyanate (TRITC)		
I-Dimethylaminonaphtalinline-5-	340 nm	525 nm
Lissamine-Rhodamine B 200 (RB 200)	575 nm	595 nm
Magdalred	540 nm	570 nm
Paraosaniline (Feulgen)	570 nm	625 nm
Phosphine 3R	465 nm	565 nm
Primuline	410 nm	550 nm
Pyronine	410 nm	540 nm
Quinacrine mustard (QM)	440 nm	510 nm
Rhodamine B	540 nm	625 nm
Acidic fuchsine	540 nm	630 nm
Stilben (SITS: Stilbenisothiosulfonacid)	365 nm	460 nm
Sulfonacide (DANS)		
Tetracycline	390 nm	560 nm
Tetramethylrhodamine	540 nm	570 nm
Thiazinred R	510 nm	580nm
Thioflavine S	430 nm	550 nm
TOTO 1 (DNA specific)	485 nm	530 nm

ACKNOWLEDGMENTS

My very grateful acknowledgments are addressed to Professor Dr. Milena Koudelka Hep of the IMT Neuchâtel for supervising my thesis and helping in many difficult situations of scientific and organizational kind. Her interest and ideas led to this kind of thesis at all.
Many thanks go to Dr. Rino E. Kunz from CSEM SA. He was my real tutor, coach and guide during the time of the thesis work. He had many ideas and was a strong help for solving problems in science and practical applications. Yet it was not easy for him to steal his time for me as his activities in Neuchâtel increased rapidly during the last 3 years, he still found time to be there for my problems to be solved.

A big thank you is for Professor Dr. Ursule Spichiger from the Center of Chemical Sensors (CCS) at Technopark in Zürich. I would like to thank also her former PhD student, Caspar Demuth, for having helped me in different ways.
I am grateful to many people of IMT, especially Luca Berdondini and Philippe Michel., having helped me on different topics, mostly in building the integrated optical ECL sensor chips.
Of course I would like to send many thanks to many coworkers of CSEM SA headquarter in Neuchâtel; namely the people of the Biochemical Sensors and Advanced Microsystems Section. Among them mostly Dr. Guy Voirin, Dr. Hui Chai-Gao and François Crevoisier for many discussions and for introducing me to the area of biochemistry as well as preparing all the bio coatings on my chips and helping to analyze the results.
Grateful thanks also go to all my coworkers of CSEM SA Zürich for their help, instruction and fellowship. Not to forget former coworkers, especially Dr. Jürg Dübendorfer, Richard Stutz and Dr. Max Wiki.

Further thanks go to OFES, OFFT and the priority program for Biotechnology that partly funded some project work.

Last but not least I would like to thank very much all the people who helped me doing this work by just being there for me in any way at whatever time.

PUBLICATIONS, TALKS AND PATENTS

- Patent: R. Kunz, M. Wiki, P. Zeller, High-Density Integrated Optical Sensors (HDIOS), First submission in Europe: 1999 February 25th, (Patent request N° 99'103'730.0; Publication date: 2000 August 30th). Extension to the USA: 2000, February 22nd, (Patent request N° 09/510,609).

- Patent: R. Kunz, G. Voirin, P. Zeller, High-Density integrated optical sensors based on amplitude effects First submission in Europe: 1999, September 15th, (Patent request N° 99'118'309.6; Publication date: 2001, Merch 21st). Extension to the USA: le 2000 September 13th. (Patent request N° 09/660,978).

- Poster presentation: Replicated Chips for Fluorescent Immunoassay, 5th SensLab99 Conference at Center for Chemical Sensors (CCS), Technopark, Zürich (September 17, 1999)

- P.N. Zeller, H. Gao, R.E. Kunz, H. Signst and Y. Karlen, Fluorescence-Based Weveguide Sensing of Oligonucleotide Tailing, 8th International Meeting on Chemical Sensors (IMCS), Basel, Switzerland, July 2-5, Abstract Book, 43, (2000)

- P.N. Zeller, G. Voirin and R.E. Kunz, Single-pad scheme for integreted optical fluorscene sensing, Biosensors and Bioelectronics, Vol.15/11-12, 591-595 (2001)

REFERENCES

[1] S.J. Scharf, G.T. Horn, H.A. Erlich, Direct cloning and sequence Analysis of enzymatically amplified genomic sequences, Science, Vol. 233, No. 4768, 1076-1078, 1986.

[2] N.L. Goddard, G. Bonnet, O. Krichevsky, A. Libchaber, Sequence Dependent Rigidity of Single Stranded DNA, Physical Review Letters, Vol. 85, No. 11, 2400-2403, 2000.

[3] L.M.S. Chang, F.J. Bollum, Molecular Biology of Terminal Transferase, CRC Critcal Reviews in Biochemistry, Vol 21, No. 1, 27-52, 1986

[4] A.L. Ghindilis, P. Atanasov, M. Wilkins, E. Wilkins, Immunosensors: Electrochemical Sensing and other Engineering Approaches, Biosensors & Bioelectronics, Vol. 13, 113-131 1998

[5] N. Kaneki, Y. Xu, A. Kumari, et al., Electrochemical Enzyme Immunoassay Using sequential Saturation Technique in a 20ul capillary: Digoxin as a Model Analyte, Analytical Chemistry, Acta 287, 253-258, 1994.

[6] C.A. Rowe-Taitt, J.P. Golden, M.J. Feldstein et al., Array Biosensor for Detection of Biohazards, Biosensors & Bioelectronics, Vol. 14, 785-794, 2000.

[7] S.R. Weinberger, T.S. Morris, and M. Pawlak, Recent Trends in Protein Biochip Technology, Pharmacogenomics, 395 – 416, 2000.

[8] V.A. Sychugov, A.V. Tishchenko, N.M. Lyndin, O. Parriaux, Waveguide Coupling Gretings for high Sensitivity biochemical Sensors, Sensors and Actuators B, 38-39, 360-364, 1997.

[9] N.F. Hartman, J. Cobb, J.G. Edwards, Optical System-on-a-Chip for chemical and biochemical Sensing: The Platform, Conference on Electro-Optic, Integrated Optic and Electronic Technologies for Chemical Detection and Identification, Boston, Massachusetts, SPIE Vol. 3537, 302-309, 1998.

[10] P.B. Oldham, A.N. Asanov, Control of Antibody-Antigen Binding or Dissociation by Electric Field, Conference on Clinical Diagnostic Systems an Technologies, San José, California, SPIE Vol. 3603, 0277-786X, 156-162 1999.

[11] A.N. Asanov, I.Y. Sarkisov, P. B. Oldham, Effect on Surface Electrostatics on Adsorption Behavior and Biospecific Interactions of DNA Oligonucleotides, Conference on Clinical Diagnostic Systems an Technologies, San José, California, SPIE Vol. 3603, 0277-786X, 170-177, 1999.

[12] H. Gao, M. Sänger, R. Luginbühl, N. Sigrist, Immunosensing with photo-immobilized Immunoreagents on planar optical Wave Guides, Biosensensors & Bioelectronics, Vol. 10, 317-328, 1995.

[13] P.B. Oldham, A.N. Asanov, V.M. Rangenkar, Surface Measuremants using Absorption/Luminescence, Encyclopedia of Anal. Chem., R.A. Meyers (Ed.), 10573-10588, J.Wiley & sons Ltd, Chichester, 2000.

[14] C.M. Ingersoll, F.V. Bright, Using Fluorescence to Probe Biosensor Interfacial Dynamics, Analytical Chemistry, Vol. 69, 403A-408A, 1997.

[15] W. Trettnak, Fundamentals of optical Detection: Luminescence, Labels, Indicators and optical Sensors, Joanneum Research, Group for Sensor-Interfaces, Graz, Austria.

[16] L.M. Levine, M.L. Michener, M.V. Toth, B.C. Howerda, Measurement of specific Protease Activity Utilizing Fluorescence Polarization, Analytical Biochemistry, Vol. 247, 83-88, 1997.

[17] M.E. Uppitsch, Optical Sensors based on Fluorescence Anisotropy, Sensors and Actuators B, Vol. 11, 499-502, 1993.

[18] W.R. Gruber, P. O'Leary, O.S. Wolfbeis, Detection of Fluorescence Lifetime based on solid State Technology and its application to optical Oxygen Sensing, Proceedings of Advances in Fluorescence Sensing Technology II, BiOS '95, San José, California, 1995.

[19] C. Deka, J.A. Steinkamp, Time-resolved Fluorescence-Decay Measurement and Analysis on single Cells by Flow Cytometry, Applied Optics, Vol. 35, No. 22, 1996.

[20] G. Valentini, C. D'Andrea, D. Comelli et al., Time-resolved DNA-reading by an Intensified CCD for ultimate Sensitivity, Optics Letters, Vol. 25, No. 22, 1648-1650, 2000.

[21] J.R. Lakowicz, I. Gryczynski, Z. Gryczynski, J.D. Dattelbaum, Anisotropy-based Sensing with Reference Fluorophores, Analytical Biochemistry, Vol. 267, 397-405, 1999.

[22] S. Blair, Y. Chen, Resonant-enhanced evanescent-Wave Fluorescence Biosensing with cylindrical optical Cavities, Applied Optics, Vol. 40, No. 4, 570-582, 2001.

[23] D. Christensen, J. Andrade, J. Wang, J. Ives, D. Yoshida, Evanescent-Wave Coupling of Fluorescence into guided Modes: FDTD Analysis. Chemical, Biochemical and Environmental Sensors, SPIE Vol. 1172, 70-74, 1989.

[24] J. Edwards, D. Ausserre, H. Hervet, F. Rondelez, Quantitative Studie of evanescent Wave Intensity Profiles Using optical Fluorescence, Applied Optics, Vol. 28, No. 10, 1881-1884, 1989.

[25] R.E. Kunz, Integrated Optics in Sensors: Advances Toward Miniaturized Systems for Chemical and Biochemical Sensing, Integrated Optical Circuits and Components, Murphy, E.J., (Ed.), Dekker, M., New York, 1999.

[26] T.M. Butler, E. Igata, S.J. Sheard, N. Blackie, Integrated optical Bragg-Grating-based chemical Sensor on a curved Input Edge Waveguide Structure, Optics Letters, Vol. 24, No. 8, 525-527, 1999.

[27] R. Srivastava, C. Bao, C. Gómez-Reino, Planar-Surface-Waveguide evanescent-Wave chemical Sensors, Sensors and Actuators A, Vol. 51, 165-171, 1996.

[28] B.J. Luff, R.D. Harris, J.S. Wilkinson et al., Integrated-optical directional Coupler Biosensor, Optics Letters, Vol. 21, No. 8, 618-620, 1996.

[29] R.G. Heideman, R.P.H. Kooyman, J. Greve, Performance of a highly sensitive optical Mach-Zehnder Interferometer Immunoassay, Sensors and Actuators B, Vol. 10, 209-217, 1993.

[30] D. Schlatter, R. Barner, Ch. Fattinger et al., The Difference Interferometer: Application as a direct Affinitysensor, Biosensors & Bioelectronics, Vol. 8, 109-116, 1993.

[31] D. Christensen, S. Dyer, J. Herron, V. Hlady, Comparison of robust Coupling Techniques for planar Waveguide Immunosensors, SPIE Vol. 1796, 20-25, 1992.

[32] D. Neuschäfer, W. Budach, E. Bär, M. Pawlak, and G. L., Duveneck, Planar Waveguides as Efficient Trensducers for Bioaffinity Sensors, Proc. SPIE, Vol. 2836, 221 – 234, 1996.

[33] R. Potzius, Th. Schneider, F.F. Bier, U. Bilitewski, W. Koschinski, Optimization of Biosensing Using Grating Couplers: Immobilization on Tantalum Oxide Waveguides, Biosensensors & Bioelectronics, Vol. 11, No. 5, 503-514, 1996.

[34] D. Kelly, K.M. Grace, X. Song et al., Integrated optical Biosensor for Detection of multivalent Proteins, Optics Letters, Vol. 24, No. 23, 1723-1725, 1999.

[35] K. Tiefenthaler, W. Lukosz, Sensitivity of Grating Couplers as integrated-optical chemical Sensors, Optical Society of America, Vol. 6, No. 2, 209-218, 1988.

[36] R.E. Kunz, W. Lukosz, Changes in fluorescence lifetimes induced by variable optical environments. Physical Review B. Vol. 21/10, 4814-4828, 1980.

[37] L. Poleretzky, J. Hamrle, B.D. MacCraith, Theory of the Radiation of Dipoles placed within a multiplayer System, Applied Optics, Vol. 39, No. 22, 3968-3977, 2000

[38] R.E. Kunz, J. Edlinger, P. Sixt, M.T. Gale, Replicated chirped waveguide gratings for optical sensing applications. Sensors and Actuators A. 46-47, 482-486, 1995.

[39] J. Dübendorfer, R.E. Kunz, E. Schürmann, G.L. Duveneck, M. Ehret, Sensing and Reference Pads for Integrated Optical Immunosensors. Journal of Biomedical Optics. Vol. 2, 391-400, 1997.

[40] R.E. Kunz, Miniature Integrated Optical Modules for Chemical and Biochemical Sensing. Sensors and Actuators B. Vol. 38-39, 13-28, 1997.

[41] M. Yoshida, K. Shigemori, M. Sugimura, M. Matano, Sensitivity Enhancement of evanescent Wave Immunoassay, Meas. Sci. Technologies, Vol. 4, 1077-1079, 1993.

[42] P. Åyräs, D.F. Geraghty, S. Honkanen et al., Thin Film Waveguide Sensors for chemical Detection, Conference on Electro-Optic, Integrated Optic and Electronic Technologies for Chemical Detection and Identification, Boston, Massachusetts, SPIE Vol. 3537, 310-316, 1998.

[43] D. Freiner, R.E. Kunz, D. Citterio, U.E. Spichiger, M.T. Gale, Integreted optical Sensors Based on Refractometry of Ion-selective Membranes, Sensors and Actuators B, Vol. 29, 277-285, 1995.

[44] R.E. Kunz, G. Duveneck, M. Ehrat, Sensing Pads for hybrid and monolithic integrated optical Immunosensors, Medical Sensors II and Fiber Optic Sensors, SPIE Vol. 2331, 1-17 1994.

[45] M. Wild, Integrated Optical Sensor Micro-Systems Based on disposable Transducers, Thesis No. 2177, Swiss Federal Institute of Technology, Lausanne, 2000.

[46] J. Dübendorfer, Replicated Integrated Optical Sensors, Thesis No. 1190, University of Freiburg, Switzerland, 1997.

[47] B. Oswald, F. Lehmann, L. Simon, E. Terpetschnig, D.S. Wolfbeis, Red Laser-Induced Fluorescence Energy Transfer in an Immunosystem, Analytical Biochemistry, Vol. 280, No. 2, 272-277, 2000.

[48] A. Neubauer, U.B. Sleytr, I. Klimant, O.S. Wolfbeis, Fiber-optic glucose biosensor using enzyme membranes with 2-D crystalline structure, Biosensors & Bioelectronics, Vol. 11, 3, 317-325, 1996.

[49] R.E. Kunz, Totally Integrated Optical Measuring Sensors. Proc. SPIE. Vol. 1587, 98-113, 1992.

[50] T.E. Plowman, W.M. Reichert, C.R. Peters, H.K. Wang, D.A. Christensen, J.N. Herron, Femtomolar sensitivity using a channel -etched thin film waveguide fluoroimmunosensor. Biosens.& Bioelectron. 11, 149-160, 1996.

[51] G.L. Duveneck, M. Pawlak, D. Neuschäfer, E. Bär, W. Budach, U. Pieles, M. Ehrat, A Novel Generation of Luminescence-based Biosensors: Single-Mode Planar Waveguide Sensors. Sensors and Actuators B. 38-39, 88-95, 1997.

[52] G. Volrin, D. Gehriger, O. Parriaux, B. Usievich, Si3N4/SiO2/Si waveguide grating for fluorescent biosensors. Proc. SPIE Vol. 3620, 109-116, 1999.

[53] A. Kolotz, C. Barzen, A. Brecht, R.D. Harris, G.R. Quigley, J.S. Wilkinson, G. Gauglitz, Sensitivity Enhancement of Transducers for total Internal Reflection Fluorescence. SPIE proceeding. Vol 3620, 345, 1999.

[54] A. Klotz, Fluoreszenzbasiertes optisches Biosensorsystem: Entwurf, Modellierung und Optimierung, Thesis, Eberhard-Karls-University, Tübingen, Germany, 1998.

[55] W. Budach, A. P. Abel, A. E. Bruno, and D. Neuschäfer, Planar Waveguides as High-Performance Sensing Platforms for Fluorescence-Based Multiplexed Oligonucleotide Hybridization Assays Analytical Chemistry, Vol 71, 3347 – 3355, 1999.

[56] M. Pawlak, E. Gtell, E. Schick, D. Anselmetti, and M. Ehrat, Functional Immobilization of Biomembrane Fragments on Planar Waveguides for the Investigation of Side-directed Ligand Binding by Surface-confined Fluorescence, Faraday Discuss, Vol. 111, 273 – 288, 1998.

[57] A.N. Asanov, W.W. Wilson, P. B. Oldham, Regenerable Biosensor Platform: A total internal reflection fluorescence cell with Electrochemical Control, Analytical Chemistry, Vol. 70, No. 6, 1156-1163, 1999.

[58] M. Ehrat, G.M. Kresbach, The Most Sensitive Biochip, or How to Find the dot of an i in an Area the Size of Switzerland, Chimia 55, 35 – 39, 2001.

[59] M. Ehrat, G.M. Kresbach, DNA and Protein Microarrays and their Contributions to Proteomics and Genomics, Chimia 54, 244 – 246, 2000.

[60] G. L. Duveneck and A.P. Abel, Review on Fluorescence-based, Planar Waveguide, Biosensors, Proc. SPIE, Vol. 3858, 59 – 71, 1999.

[61] W.M. Reichert, J.T: Ives, P.A. Suci, V. Hlady, Excitation of Fluorescent Emission from Solutions at the Surface of Polymer thin-Film Waveguides: An integrated Optics Technique for the Sensing of Fluorescence at the Polymer/Solution Interface, Applied Spectroscopy, Vol. 41, No. 4, 636-640, 1987.

[62] Y. Zhou, P.J.R. Layboum, J.V: Magill, R.M. De la Rue, An evanescent Fluorescence Biosensor Using ion-exchanged buried Waveguides and the Enhancement of Peak Fluorescence, Biosensors & Bioelectronics, Vol. 6, 595-607, 1991.

[63] I.M. Walczak, W.F. Love, T.A. Cook, R.E. Slovacek, The Application of evanescent Wave Sensing to a high-sensitivity Fluoroimmunoassay, Biosensors & Bioelectronics, Vol. 7, 39-48, 1992.

[64] P.N. Zeller, H. Gao, R.E. Kunz, H. Sigrist and Y. Karlen, Fluorescence-Based Waveguide Sensing of Oligonucleotide Tailing, 8th International Meeting on Chemical Sensors (IMCS), Basel, Switzerland, July 2-5, Abstract Book, 43, 2000.

[65] P.N. Zeller, G. Volrin and R.E. Kunz, Single-pad scheme for integrated optical fluorscene sensing, Biosensors and Bioelectronics, Vol.15/11-12, 591-595 2001

[66] S.-W. Kang, K. Sasaki, H. Minamitani, Sensitivity Analysis of a thin-Film optical Waveguide biochemical Sensor Using evanescent Field Absorption, Applied Optics, Vol. 32, No. 19, 3544-3549, 1993.

[67] S.B. Mendes, S.S. Saavedra, On probing molecular Monolayers: A spectroscopic optical Waveguide Approach of ultra-Sensitivity, Optics Express, Vol. 4, No. 11, 449-456, 1999.

[68] H. Gnewuch, N. Renner, Mode-Independent Attenuation in evanescent-Field Sensors, Applied Optics, Vol. 34, No. 9, 1473-1483, 1995.

[69] T. Okamoto, M. Yamamoto, I. Yamaguchi, Optical Waveguide Absorption Sensor Using a single Coupling Prism, Optical Society of America a, Vol. 17, No. 10, 1880-1886, 2000

[70] G.C. Flaccabrino, N.F. de Rooij, M. Koudelka-Hep, On-Chip Generation and Detection of Electrochemiluminescence,

[71] E. L'Hostis, P.E. Michel, G.C. Flaccarbino, D.J. Strike, N.F. de Rooij, M. Koudelka-Hep, Microreactor and electrochemical detectors fabricated using Si and EPON SU-8, Sensors and Actuators B, Vol. B64, No. 1-3; 156-162, 2000.

[72] Ch. Hafner, Getting Started with Max-1, J. Wiley & Sons Ltd, Chichester, 1998.

[73] W.B. Dandliker, V.A. de Saussure, Fluorescence Polarisation in Immunochemistry, Immunochemistry No. 7, 799-805, 1970

[74] G. Voirin, H. Sigrist, W. Haasnoot, B. Ipema et al., Measurement of Antibiotics in Contaminated Raw Milk, Centre Suisse d'electronique et de microtechnique SA, Neuchâtel, Switzerland, Annual Report, 47, 2000.

[75] R. Roychoudhury and R. Wu, Terminal transferase-catalyzed addition of nucleotides to 3'termini of DNA, Methods Enzymol, Vol. 65(1), 43-62 1980.

[76] J. J. Storhoff, A. A. Lazarides, C. A. Mirkin, R. L. Letsinger, R. C. Mucic, and G. C. Schatz, What controls the optical properties of DNA-linked gold nanoparticle assemblies, Journal of the American Chemists Society, 122, 4640-50, 2000.

[77] Analysis and Cloning of Eukaryotic Genomic DNA, Tm = 1.5°C + 16.6 (log [Na+]) + ...some terms to neglect - (600/L) =
= 81.5 + 16.6 (log [Na+]) - (600/30) = 47.8°C
[Na+] is the concentration of sodium in reaction buffer (valid for 0.01M to 0.4M). l is the length of the hybrid in base pairs.

[78] P. N. Zeller, Replicated Chips for Fluorescent Immunoassay, Poster presentation, 5th SensLab99 Conference at Center for Chemical Sensors (CCS), Technopark, Zürich 1999

[79] G. J. Mohr, I. Klimant, U.E. Spichiger, O.S. Wolfbeis, Fluoro Reactands and dual Luminophore Referencing: A Technique to optically Measure Amines, Analytical Chemistry, Vol. 73, 1053-1056, 2001.

[80] R. Eckert, M. Fryland, H. Heinzelmann, N.F. de Rooij et al., Optical Super-Resolution with Microfabricated Probes, Centre Suisse d'electronique et de microtechnique SA, Neuchâtel, Switzerland, Annual Report, 44, 2000.

CURRICULUM VITAE

of Philipp Nicolas Zeller

1971, April 3rd:	Birth in Basel, Switzerland
Mother:	Erika, maiden name: Meinhardt
Father:	Rudolf Jakob
1976 – 1978	Kindergarten in Binningen, Baselland, Switzerland
1978 – 1980	Elementary school in Binningen, Baselland, Switzerland
1980 – 1982	Elementary school in Basel, Switzerland
1982 – 1990	Gymnesium in Basel, Switzerlend
1989	Preparation school for pilots (FVS 1)
1990	Matura, Type B (German, Latin, English, French)
1990	Preparation school for pilots (FVS 2)
1990	Practice at Suter & Suter AG, Architekturbüro, Basel
1991	Military service, reaching the degree of a Corporal
1991 – 1997	Studies in Physics at the Swiss Federal Institute of Technology (ETH), Zürich, Switzerland
1994	Advanced federal school for pilots (FWB 1, Aerobatics)
1995	Advanced federal school for pilots (FWB 2, CVR)
1995 – 1996	Parallel courses in Swedish at the University of Zürich, Switzerland
1995 – 1997	Extra work at the Aerospace Project Development Group (Arbeitsgruppe für Luft und Raumfahrt, ALR) in Zürich, Switzerland
1997	ETH Diploma Dissertation at the Paul Scherrer Institute (PSI), Villingen, end Klinik im Park Hospital, Zürich, Switzerland, entitled: Comparison of Therapy Planning for Eye Tumors Using Protons and the Leksell Gamma Knife
1998	Promotion to a military Sergeant (Wachtmeister)
1998 - 2001	Research for a PhD thesis at Centre Suisse d'Electronique et de Microtechnique (CSEM) SA, Zürich and Neuchâtel, Switzerland, entitled: Fluorescence Based Integrated Optical Biosensors
since 2001	Work as a project leader of a biomedical research project at Centre Suisse d'Electronique et de Microtechnique (CSEM) SA, Zürich, Switzerland